Kent Academic Repository

Steer, Nadine G., Bardo, Ameline, Davies, Thomas W., Rosas, Antonio, Skinner, Matthew M. and Kivell, Tracy L. (2025) *Functional morphology of the scaphoid in extant African apes, humans and fossil hominins.* American Journal of Biological Anthropology, 188 (4). ISSN 2692-7691.

Downloaded from

https://kar.kent.ac.uk/112314/ The University of Kent's Academic Repository KAR

The version of record is available from

https://doi.org/10.1002/ajpa.70157

This document version

Publisher pdf

DOI for this version

Licence for this version

CC BY-NC (Attribution-NonCommercial)

Additional information

Versions of research works

Versions of Record

If this version is the version of record, it is the same as the published version available on the publisher's web site. Cite as the published version.

Author Accepted Manuscripts

If this document is identified as the Author Accepted Manuscript it is the version after peer review but before type setting, copy editing or publisher branding. Cite as Surname, Initial. (Year) 'Title of article'. To be published in ***Title of Journal*** , Volume and issue numbers [peer-reviewed accepted version]. Available at: DOI or URL (Accessed: date).

Enquiries

If you have questions about this document contact ResearchSupport@kent.ac.uk. Please include the URL of the record in KAR. If you believe that your, or a third party's rights have been compromised through this document please see our Take Down policy (available from https://www.kent.ac.uk/guides/kar-the-kent-academic-repository#policies).

American Journal of Biological Anthropology

WILEY

AMERICAN JOURNAL OF
BIOLOGICAL ANTHROPOLOGY
The Official Journal of the American Association of Biological Anthropologists

RESEARCH ARTICLE OPEN ACCESS

Functional Morphology of the Scaphoid in Extant African Apes, Humans and Fossil Hominins

Nadine G. Steer[1,2] | Ameline Bardo[3,4] | Thomas W. Davies[5] | Antonio Rosas[6] | Matthew M. Skinner[4,7] |
Tracy L. Kivell[4,7]

[1]School of Anthropology & Conservation, University of Kent, Canterbury, UK | [2]Department of Pathology and Anatomical Sciences, University of Missouri, Columbia, USA | [3]Département Homme et Environnement, Musée de l'Homme, UMR 7194 - HNHP, CNRS-MNHN, Paris, France | [4]Department of Human Origins, Max Planck Institute for Evolutionary Anthropology, Leipzig, Germany | [5]Department of Evolutionary Biology, University of Vienna, Vienna, Austria | [6]Paleoanthropology Group, Museo Nacional de Ciencias Naturales-Consejo Superior de Investigaciones Científicas (CSIC), Madrid, Spain | [7]Centre for the Exploration of the Deep Human Journey, University of the Witwatersrand, Johannesburg, South Africa

Correspondence: Nadine G. Steer (ngsc8v@missouri.edu)

Received: 5 January 2025 | **Revised:** 20 October 2025 | **Accepted:** 29 October 2025

Funding: This project has received funding from the European Research Council (ERC) under the European Union's Horizon 2020 research and innovation programme (grant agreement No. 819960) and the GREAT Scholarship funded by the British Council and University of Kent (NGS). This work was partially funded by the Spanish Ministry of Science Innovation and Universities through the projects PID2021-122356NB-I00 to A.R.

Keywords: *Australopithecus* | carpal | fossil *Homo* | geometric morphometrics | wrist

Palabras Clave: Australopithecus | carpo | Homo fósil | morfometría geométrica | muñeca

Mots clés: os du carpe | fossiles *Homo* | morphométrie géométrique | poignet | australopithèque

ABSTRACT

Objectives: The morphology of the hominoid scaphoid has played a key role in functional and evolutionary hypotheses related to the emergence of hominin bipedalism and tool use. However, the scaphoid's complex morphology is challenging to comparatively analyze via traditional 2D linear measurements. This study quantifies scaphoid morphology utilizing 3D geometric morphometrics (3D GM) in African apes, humans and extinct hominins to provide a more holistic functional understanding of scaphoid morphology.

Materials and Methods: We use 3D GM, including anatomical and sliding semi-landmarks, to quantify scaphoid morphology in a comparative sample of African apes (*Gorilla*, *Gorilla beringei*, *Pan paniscus* and *Pan troglodytes*) ($N=54$), extant and fossil *Homo sapiens* ($N=20$) and nine fossil hominin scaphoids from *Australopithecus* sp., *Australopithecus sediba*, *Homo naledi* and Neandertals.

Results: Principal component analysis indicates that extant species can be distinguished by differences in scaphoid shape that are consistent with variation in hand use during locomotion and manipulation. The australopith scaphoids plot between the African ape and modern human distributions, whereas *H. naledi* falls between *Gorilla* and human distributions.

Discussion: Results confirm previous studies describing differences between extant African apes and modern human scaphoids that were interpreted as advantageous for knuckle-walking and forceful manipulation, respectively. However, we highlight greater variation between *Pan* and *Gorilla* than previously recognized. The fossil hominin scaphoids present differing mosaics of joint orientation and shape, creating a distinct overall morphology in each hominin species. This may reflect differing functional pressures acting upon hominin wrists resulting from disparate combinations of locomotor and manipulative behaviors.

This is an open access article under the terms of the Creative Commons Attribution-NonCommercial License, which permits use, distribution and reproduction in any medium, provided the original work is properly cited and is not used for commercial purposes.

© 2025 The Author(s). *American Journal of Biological Anthropology* published by Wiley Periodicals LLC.

26927691, 2025, 4, Downloaded from https://onlinelibrary.wiley.com/doi/10.1002/ajpa.70157 by NICE, National Institute for Health and Care Excellence, Wiley Online Library on [09/12/2025]. See the Terms and Conditions (https://onlinelibrary.wiley.com/terms-and-conditions) on Wiley Online Library for rules of use; OA articles are governed by the applicable Creative Commons License

RESUMEN

Objetivos: La morfología del escafoides de los hominoideos ha desempeñado un papel clave en las hipótesis funcionales y evolutivas relacionadas con la aparición del bipedismo y el uso de herramientas. Sin embargo, la compleja morfología del escafoides representa un desafío para su análisis comparativo mediante mediciones lineales tradicionales en 2D. Este estudio cuantifica la morfología del escafoides utilizando morfometría geométrica en 3D (3D GM) en simios africanos, humanos y homininos extintos, con el fin de proporcionar una comprensión funcional más integral de su morfología.

Materiales y Métodos: Utilizamos morfometría geométrica en 3D, incluyendo puntos de referencia anatómicos(landmarks) y semi-landmarks de referencia, para cuantificar la morfología del escafoides en una muestra comparativa de simios africanos (*Gorilla gorilla*, *Gorilla beringei*, *Pan paniscus* y *Pan troglodytes*) ($N = 54$), humanos modernos y fósiles (*Homo sapiens*) ($N = 20$) y nueve escafoides fósiles de homínidos de *Australopithecus* sp., *Australopithecus sediba*, *Homo naledi* y Neandertales.

Resultados: El análisis de componentes principales indica que las especies actuales pueden distinguirse por diferencias en la forma del escafoides, las cuales son consistentes con la variación en el uso de la mano durante la locomoción y la manipulación. Los escafoides de los australopitecos se sitúan entre las distribuciones de simios africanos y humanos modernos, mientras que *H. naledi* se posiciona entre *Gorilla* y *H. sapiens*.

Discusión: Los resultados confirman estudios previos que describen diferencias entre los escafoides de simios africanos actuales y los humanos modernos, interpretadas como ventajosas para la marcha sobre los nudillos y la manipulación con fuerza, respectivamente. Sin embargo, destacamos una mayor variación entre *Pan* y *Gorilla* de la que se había reconocido anteriormente. Los escafoides fósiles de homininos presentan diferentes mosaicos de caracteres en la orientación y forma de las articulaciones, lo que da lugar a una morfología general distinta en cada especie. Esto podría reflejar distintas presiones funcionales que actúan sobre las muñecas de los homininos, como resultado de combinaciones dispares de comportamientos locomotores y manipulativos.

RÉSUMÉ

Objectifs: La morphologie des scaphoïdes des hominoïdes a joué un rôle clé dans les hypothèses fonctionnelles et évolutionnaires liées à l'émergence de la bipédie et de l'utilisation d'outils chez les hominines. Cependant, la morphologie complexe du scaphoïde rend difficile son analyse comparative à l'aide de mesures linéaires 2D traditionnelles. Cette étude quantifie la morphologie du scaphoïde à l'aide de la morphométrie géométrique 3D (3D GM) chez les grands singes africains, les humains et les hominines éteints afin de fournir une compréhension fonctionnelle plus holistique de sa morphologie.

Matériels et Méthodes: Nous utilisons de la morphométrie géométrique 3D, comprenant des points anatomiques de références (landmarks) et des semi-landmarks de références (sliding semi-landmarks), afin de quantifier la morphologie du scaphoïde dans un échantillon comparatif de grands singes africains (*Gorilla gorilla, Gorilla beringei, Pan paniscus* et *Pan troglodytes*) ($N = 54$), d'*Homo sapiens* actuels et fossiles ($N = 20$) et de neuf scaphoïdes fossiles d'hominines appartenant aux espèces *Australopithecus* sp., *Australopithecus sediba*, *Homo naledi* et Néandertaliens.

Résultats: L'analyse en composantes principales indique que les espèces actuelles peuvent être différenciées par des différences dans la forme du scaphoïde, qui correspondent à des variations dans l'utilisation de la main lors de la locomotion et de la manipulation. Les scaphoïdes des australopithèques se situent entre les distributions morphologiques des grands singes africains et des humains anatomiquement modernes, tandis que *H. naledi* se situe entre les distributions des gorilles et des humains.

Discussion: Les résultats confirment les études précédentes décrivant des différences entre les scaphoïdes des grands singes africains actuels et des humains modernes, qui ont été interprétées comme avantageuses, respectivement, pour la marche sur les phalanges (et la manipulation avec force). Cependant, nous soulignons une plus grande variation entre *Pan* et *Gorilla* que ce qui avait été reconnu auparavant. Les scaphoïdes des hominines fossiles présentent différentes mosaïques de caractères en termes d'orientation et de forme des articulations, créant une morphologie globale distincte pour chaque espèce d'hominines. Cela peut refléter différentes pressions fonctionnelles exercées sur les poignets des hominines, résultant de combinaisons disparates de comportements locomoteurs et manipulateurs.

1 | Introduction

The scaphoid is a carpal bone on the radial side of the wrist that spans both the proximal and distal rows of the carpus. In African apes and modern humans, as well as some strepsirrhines, the os centrale is fused to the scaphoid and articulates distoradially with the trapezium and trapezoid, distally to the capitate, proximally to the radius, and ulnarly with the lunate (Kivell and Begun 2007; Kivell 2016). The scaphoid plays a key functional role in dissipating forces across the wrist accrued from both locomotor and manipulative behaviors (Kauer and de Lange 1987; Caley M. Orr 2018; Wolfe et al. 2006) and, together with its associated soft tissues, contributes to stability and range of motion within the radial carpus (Berger 1997; Moggi-Moojen et al. 2003). Scaphoid-centrale fusion is considered a synapomorphy of the African ape and human clade (Begun 2004; Kivell and Begun 2007; Sarmiento 1988). This fusion is often interpreted as a functional adaptation for ameliorating mechanical loads experienced in knuckle-walking behaviors in African apes (Püschel et al. 2020; Tocheri 2007) and considered a possible phylogenetic vestige (Richmond and Strait 2001) or exaptation to withstand shear stresses accrued during manipulative activities (Marzke 1971). As such, variation in external morphology of the scaphoid has featured prominently in hypotheses about the origin of hominin bipedalism (Begun 2004; Kivell and Schmitt 2009; Caley M. Orr 2005; Richmond et al. 2001; Püschel et al. 2020) and the evolution of hominin tool-related behaviors (Marzke 1971, 2013; Tocheri 2007; Tocheri et al. 2008; Kivell, Rosas, et al. 2018). To date, scaphoid morphology has primarily been studied using 2D approaches (Trinkaus 1989; Hamrick 1997; Kivell et al. 2011; Kivell et al. 2015; Kivell, Churchill, et al. 2018; Kivell, Rosas, et al. 2018) or using basic 3D approaches (Tocheri 2007; Kibii et al. 2011). However, given the complexity of scaphoid morphology, 3D geometric morphometric methods are ideal and have yet to be applied. This study conducts a comprehensive examination of the external morphology of the African ape, modern human and fossil hominin scaphoid to understand its functional morphology and to inform the evolution of wrist and hand use in Plio-Pleistocene hominins.

1.1 | Functional Morphology of African Ape Scaphoids

In African apes, the most frequent form of locomotion is knuckle-walking alongside varying frequencies of arboreal locomotion depending on the habitat type, species and sex (D. M. Doran 1993, 1996, 1997; Drummond-Clarke et al. 2022; Drummond-Clarke et al. 2024; Hunt 1991; Remis 1995; Sarringhaus et al. 2014; van Lawick-Goodall 1968). Knuckle-walking requires the wrist to be in slight extension (Finestone et al. 2018; Thompson 2020) with the forces acting on the scaphoid being mainly generated from compressive loads running distoproximally via the long axis of the second or third metacarpal depending on the hand posture adopted (Matarazzo 2013; Wunderlich and Jungers 2009; Samuel et al. 2018; Thompson 2020). During arboreal activities, apes will grasp the substrate with both an adducted and abducted thumb and the wrist posture will vary depending on the size of the substrate and activity, ranging from highly flexed to extended (Neufuss et al. 2017; Sarmiento 1988). In addition, non-human apes engage in manipulative behaviors using precision grips, power grips, and interdigital braces that can recruit the thumb in both adducted and abducted positions, potentially altering the stress experienced by the scaphoid (Bardo et al. 2017; Boesch and Boesch 1990; Christel 1993; Marzke et al. 2015; Neufuss et al. 2019). It is assumed that loads incurred by the scaphoid, and hand overall, during manipulation are lower than those incurred during locomotion, although manipulative loads have not been quantified in African apes (reviewed in Kivell et al. 2023).

Aspects of African ape scaphoid morphology are considered advantageous to limiting extension at the radiocarpal and midcarpal joints, providing greater stability during knuckle-walking (e.g., Begun 2004; Jenkins and Fleagle 1975; Richmond et al. 2001; Thompson 2020; Püschel et al. 2020). Some of these morphological features include the presence of a scaphoid beak along the dorsal edge of a large radial facet that is thought to help dissipate unidirectional compressive loads, as well as a 'closed' distoulnar border of the capitate facet that facilitates close-packing of the scaphoid's centrale portion with the capitate and trapezoid to reduce shear stress experienced during knuckle-walking (Begun 2004; Corruccini 1978; Caley M. Orr 2018; Richmond et al. 2001; Sarmiento 1988; Tallman 2012; Tocheri 2007). Furthermore, kinematic analyses in *Pan* show that the scaphoid is part of the "screw-clamp mechanism" of the carpus that allows the proximal and distal carpal rows to rotate in unison, creating an overall structure that is relatively more stable than that of *Pongo* (Caley Michael Orr 2010). African apes also generally share a palmarly-projecting tubercle and distopalmarly-oriented trapezium-trapezoid facet that reflect a deep carpal tunnel for powerful wrist and digit flexor muscles (Taverne et al. 2018; R. H. Tuttle 1969). However, many of these morphological features are variable in their presence or degree of expression across different African ape species or are found in other primates, and thus their functional significance, if any, remains unclear (Lewis 1989; Kivell 2007; Kivell and Begun 2007; Kivell and Schmitt 2009).

1.2 | Functional Morphology of the Human Scaphoid

Most modern humans rarely use their hands for locomotor behaviors (but see Kraft et al. 2014) and instead typically grasp and manipulate objects using a variety of (forceful) pad-to-pad precision grips, power grips, including power-squeeze grips, and in-hand manipulation (Key and Dunmore 2015; Key et al. 2017; Marzke 1997; Napier 1956). The thumb is larger and capable of generating greater force and torque than that of other hominoids, which facilitates opposition to the fingers (Marzke et al. 1992; Marzke et al. 1999; Napier 1960). Compared with African apes, the human scaphoid is oriented in a more supinated position, as part of an overall reorientation of the radiocarpal complex (Orr et al. 2013; Tocheri 2007, Kivell 2015). The human scaphoid has a shorter, more buttressed tubercle, broader trapezium-trapezoid articulation that extends onto a more radially projecting scaphoid tubercle, and an open distoulnar border to the capitate facet (Kivell 2016; Orr et al. 2013; Tocheri 2007). Together, these changes have been interpreted as better accommodating high radioulnar loading and shear forces from forceful and frequent thumb use in manipulative behaviors (Tocheri et al. 2003; Tocheri 2007).

1.3 | Fossil Hominin Scaphoids

Relative to other hand bones, there are few hominin scaphoids discovered thus far in the Plio-Pleistocene fossil record. There are currently only three known australopith scaphoids; we include two in our study while the third, associated with StW 573, remains unpublished (Crompton et al. 2018). StW 618 is a complete scaphoid discovered at Sterkfontein (Member 4), South Africa, dating to 2.0–2.6 Ma (Pickering and Herries 2020; but see Granger et al. 2022) and is currently attributed to *Australopithecus* sp. (Kibii et al. 2011). The initial analysis of its morphology, including a 3D analysis of facet orientation and surface area, describes it as primitive in overall morphology, lacking the shared derived features of Neandertals and modern humans. Instead, it is most

26927691, 2025, 4, Downloaded from https://onlinelibrary.wiley.com/doi/10.1002/ajpa.70157 by NICE, National Institute for Health and Care Excellence, Wiley Online Library on [09/12/2025]. See the Terms and Conditions (https://onlinelibrary.wiley.com/terms-and-conditions) on Wiley Online Library for rules of use; OA articles are governed by the applicable Creative Commons License

similar to that of African apes in having, for example, a distally "closed" capitate border and a trapezium-trapezoid facet that does not expand radially and palmarly onto the tubercle (Kibii et al. 2011). The associated right hand of *A. sediba* MH2 from Malapa, South Africa (1.98 Ma; Pickering et al. 2011) includes a complete scaphoid (U.W. 88-158), missing only a small fragment from the tip of its tubercle (Berger et al. 2010; Kivell et al. 2011). The MH2 scaphoid is described as having a mosaic morphology, with a more ape-like 'closed' distoulnar border of the capitate facet but a human-like trapezium facet that extends onto the tubercle (Kivell et al. 2011; Kivell, Churchill, et al. 2018).

We also include in our sample fossil scaphoids from the genus *Homo*. The nearly complete right hand (Hand 1) of *Homo naledi* from the Dinaledi Chamber of the Rising Star cave system, South Africa (241–335 Ka; Dirks et al. 2017; Robbins et al. 2021) includes a well-preserved scaphoid (U.W. 101-1726). The Lesedi Chamber within the same cave system also preserves a complete right scaphoid (U.W. 102a-117), in association with a partial lunate and complete capitate (Hawks et al. 2017). Three-dimensional morphometric analyses of the joint orientation and surface area show that both *H. naledi* scaphoids share a large trapezium facet that extends onto the tubercle as in modern humans and Neandertals, but that their overall morphology is distinct from that of other hominins, occupying their own morphospace (Hawks et al. 2017; Kivell et al. 2015).

Both Neandertals and early *Homo sapiens* engaged regularly in a variety of complex tool-related behaviors and manipulative activities (e.g., Aranguren et al. 2018; Abrams et al. 2024; Soressi et al. 2013; Arrighi et al. 2020) and are characterized by hand morphology that is generally similar to that of recent *H. sapiens* (Tocheri et al. 2008; Kivell et al. 2023), with Neandertals showing some distinct features (e.g., Bardo et al. 2020; Niewoehner et al. 1997; Trinkaus 1989). Our Neandertal sample includes two well-preserved scaphoids (SD 258 and SD 1243) from El Sidrón in Asturias, Spain (~49 Ka; Wood et al. 2013). Both scaphoids are similar in morphology, although SD 258 preserves a distinct, but fused, os centrale portion along the distal border (Kivell, Rosas, et al. 2018). In addition, we include scaphoids from three Neandertal skeletons: Kebara 2, thought to be male (60 Ka; Schwarcz et al. 1989), Tabun C1, considered female (~30 Ka; Schwarcz et al. 1998), and Le Régourdou 1 of indeterminate sex (~91 Ka; Delpech 1996). Previous morphological analyses of these Neandertal specimens show that all exhibit typical Neandertal morphology, with shared derived morphology with *H. sapiens* such as a large trapezium facet, an open capitate facet, and a robust tubercle (Kivell, Rosas, et al. 2018; Orr et al. 2013; Tocheri et al. 2008). Finally, our fossil *H. sapiens* sample includes two individuals that are both considered male: Arene Candide 2 from Finale Liguria, Liguria, Italy (11,650–11,550 BP; Sparacello et al. 2018, Sparacello et al. 2021) and Barma Grande 2 from Balzi Rossi, Liguria, Italy (~24 Ka; Churchill and Formicola 1997).

This study represents a proof of concept in applying 3D GM methods to investigate scaphoid morphology in extant African apes, modern humans, and fossil hominins. It is expected that there will be differences in the shape and orientation of the scaphoid articular facets and tubercle that, based on previous studies, will distinguish African apes from modern humans, with implications that the differing morphology is related to functional differences between locomotor versus manipulative behaviors. As joint shape and orientation influence the range of motion and stability of the wrist, the investigation of scaphoid morphology in extant hominids with known behaviors provides a strong comparative framework for the functional interpretation of hominin wrist evolution. However, there is difficulty in assessing functional features of morphology utilizing solely linear measurements given that the scaphoid has a complex and variable shape across and within hominid taxa and articulates with multiple bones (Ceri et al. 2004; Kauer and de Lange 1987). This study utilizes 3D landmark-based geometric morphometrics (3D GM) to quantify variation in overall scaphoid morphology, as well as differences in articular facet shape and joint orientation, with the expectation that GM will provide a better discrimination of the shape differences across extant species than that provided in previous 2D (Kivell et al. 2015, 2011; Kivell, Churchill, et al. 2018; Kivell, Rosas, et al. 2018) and 3D studies (Tocheri et al. 2007). We expect that 3D GM will also provide better discrimination among African ape taxa than found in previous studies due to varying frequencies of terrestrial and arboreal locomotor behaviors and differences in knuckle-walking postures and biomechanics (see above; reviewed in Kivell et al. 2023). Among fossil hominins, based on previous morphological descriptions, it is expected that *Australopithecus* sp. StW 618 will share morphological similarity with the African apes and that Neandertals will fall closest to *H. sapiens*. We use this first 3D GM analysis of scaphoid morphology to shed new light on the mosaic morphologies of *A. sediba* and *H. naledi*.

2 | Materials and Methods

2.1 | Study Sample

As presented in Table 1, our extant sample comprises *H. sapiens* ($n=20$), *Gorilla gorilla* ($n=24$), *Gorilla beringei* ($n=5$), *Pan troglodytes* ($n=19$) and *Pan paniscus* ($n=7$), including females, males and specimens of unknown sex, which are curated at several institutions outlined in Table S1. Representative individuals displaying the typical morphology for most taxa are displayed in Figure 1. All specimens are adult with no visible pathologies. Both right and left scaphoids are included, but only one from each extant individual (although both sides were included for fossil taxa when preserved). All non-human apes were wild caught and, among the *Gorilla* sample, none of the specimens

TABLE 1 | Summary of extant taxa.

Species	*N*	Male	Female	Unknown sex
Homo sapiens	18	2	8	8
Gorilla gorilla	24	12	8	4
Gorilla beringei	5	1	3	1
Pan troglodytes	19	9	7	3
Pan paniscus	7	2	5	—

26927691, 2025, 4, Downloaded from https://onlinelibrary.wiley.com/doi/10.1002/ajpa.70157 by NICE, National Institute for Health and Care Excellence, Wiley Online Library on [09/12/2025]. See the Terms and Conditions (https://onlinelibrary.wiley.com/terms-and-conditions) on Wiley Online Library for rules of use; OA articles are governed by the applicable Creative Commons License

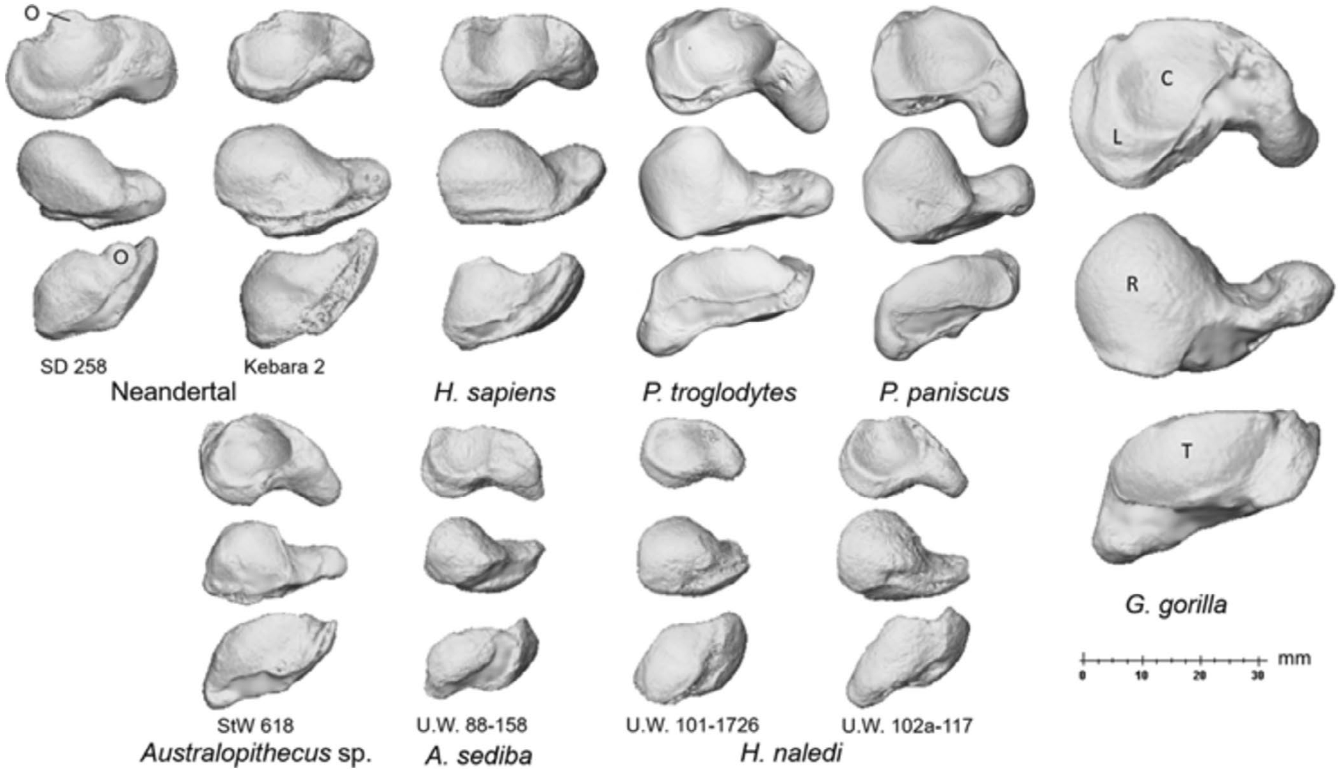

FIGURE 1 | MicroCT-derived surface models of extant taxa and fossil hominins shown in distal (top), proximal (middle) and dorsal (bottom) views. For reference, the articular facets are labeled on the *Gorilla* specimen, indicating the capitate (C), lunate (L), radius (R), and trapezium-trapezoid (T). The unusual os centrale (O) portion of the El Sidrón SD 258 specimen is highlighted. All specimens are shown to scale. Representative individuals for each extant taxon are University of Florence 4865 (*H. sapiens*), MPI-TC 11781 (*P. troglodytes*), MRAC 29045 (*P. paniscus*) and PC MER 300 (*G. gorilla*).

had a prepollex that was fused to the scaphoid tubercle, which is common in this taxon.

Our modern *H. sapiens* sample includes individuals from several geographical and temporal contexts (Table S1). The majority of our sample ($n = 8$) derives from a late 19th-century cemetery in Inden, Germany curated at Johann-Friedrich-Blumenback-Institute for Zoology and Anthropology, Georg-August University, Göttingen, Germany (Grosskopf 2015). Our modern *H. sapiens* sample also includes two individuals from the Municipal Cemetery of Syracuse, Italy excavated in 1909, and one Yámanas individual from Tiera del Fuego, all of which are curated at the National History Museum, University of Florence, Italy (Moggi-Cecchi and Roscoe 2014). Two individuals are curated at the Musée de l'Homme Paris, France and are from the Democratic Republic of the Congo and the Philippines. Two individuals are from a medieval St. Gregory's priory (13th–16th century) excavated between 1988 and 1991 in Canterbury, UK and curated at the University of Kent, Canterbury, UK (Hicks and Hicks 2001). Finally, three individuals are curated at the Duckworth Collection, University of Cambridge where one comes from southwestern, USA and two from Chatham Islands, UK. All specimens derive from collections accessible for research and were microCT scanned or surface scanned with permission from the respective curatorial institutions.

The fossil hominin specimens, as described above, include a geographically- and temporally diverse sample, including early australopiths, *H. naledi* and Neandertals (Table 2). We include the two fossil *H. sapiens* specimens (Arene Candide 2 and Barme Grande 2) within our extant *H. sapiens* sample.

2.2 | Micro-Computed Tomography, Surface Scanning and Surface Models

The digital data for our sample derives primarily from high-resolution microCT scanning at different institutions, with a resolution range of 0.035–0.048 mm, using a voltage of 100–160 kV and 100–140 μA with a 0.2- to 0.5- mm brass or copper filter. A few extant specimens and the Le Régourdou 1 Neandertal specimen derived from surface laser scans using a high-quality resin cast of the original specimen and a desktop laser digitizer (Cyberware Model 15). We outlined the details of the curatorial institution, samples and methods of scanning with Table S2.

Surface models were generated from an isosurface derived from microCT and surface scan data using Avizo 6.3 (FEI Visualization Sciences Group, Berlin, Germany). Any internal bone structure was removed using a custom script in Meshlab (Cignoni et al. 2008). The surface models were then cleaned in Geomagic Wrap 2021 (3D Systems Inc., United States), where minor deformities on the surface such as small pits were removed using the defeature tool, and holes on the surface were filled using the hole fill tool on all specimens (Figure 2). Despite different methods of scan acquisition, previous studies have demonstrated minimal effects of scanning modality on 3D morphometric analyses (e.g., Tocheri et al. 2011; Robinson

26927691, 2025, 4, Downloaded from https://onlinelibrary.wiley.com/doi/10.1002/ajpa.70157 by NICE, National Institute for Health and Care Excellence, Wiley Online Library on [09/12/2025]. See the Terms and Conditions (https://onlinelibrary.wiley.com/terms-and-conditions) on Wiley Online Library for rules of use; OA articles are governed by the applicable Creative Commons License

TABLE 2 | Summary of fossil sample.

Species	*N*	Specimen	Institution	Side
Homo naledi	2	U.W. 101-1726*, U.W. 102a-117	UW	R
Neandertals	5	SD 258, SD 1243, Kebara 2, Tabun C1*, Le Régourdou 1	CSIC, TAU, MPP, MNP	L
Australopithecus sp.	1	StW 618	UW	L
Australopithecus sediba	1	U.W. 88-158	UW	R
Homo sapiens	2	Arene Candide Barma Grande	MAF MNPBR	R, L R, L

Note: '*' indicates part of the morphology was reconstructed.
Abbreviations: CSIC, Museo Nacional de Ciencias Naturales; L, left; MAF, Museo Archeologico del Finale; MNP, Musée national de Préhistoire; MNPBR, Museo Nazionale Preistorico dei Balzi Rossi; MPP, Museum Perigord Perigueux; R, right; TAU, Sackler School of Medicine, Tel Aviv University; UW, University of the Witwatersrand.

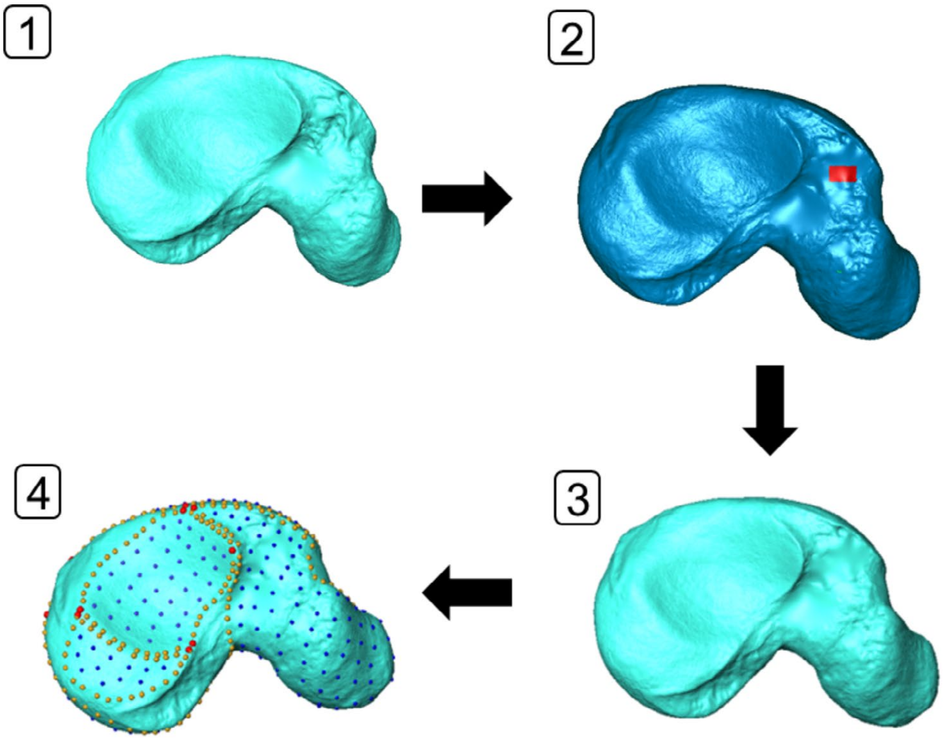

FIGURE 2 | Methodological steps to scaphoid shape analysis. (1) a surface model of the external shape is created from either microCT or surface scans; (2) when required, the surface is smoothed or holes are filled to create (3) a surface model appropriate for landmarking; (4) Main anatomical landmarks (red) and curve semilandmarks (yellow) are placed on each specimen individually, while surface semilandmarks (blue), are placed on a template specimen before being projected on to the other specimens.

and Terhune 2017; Shearer et al. 2017; Waltenberger et al. 2021; Bowland et al. 2021).

Two fossil specimens were not completely preserved and therefore multiple reconstructions of the unpreserved morphology were manually generated using the sculpt knife tool on the available facets or features in Geomagic Wrap 2021 (3D Systems Inc., United States). These were reconstructed following the Freeform modeling protocol in (Loeffelbein et al. 2015). The *H. naledi* scaphoid associated with Hand 1 from the Dinaledi Chamber (U.W. 101-1726) is missing the palmar tip of the tubercle and the base of the tubercle is eroded. For this specimen, reconstruction of the missing morphology was based on the complete *H. naledi* scaphoid from the Lesedi Chamber (U.W. 102a-117). By superimposing the two scaphoids, the surface of the incomplete U.W. 101-1726 scaphoid was manually added and deformed, whilst toggling the visibility of the Lesedi U.W. 102a-117 material off and on. The U.W. 101-1726 trapezium-trapezoid facet was extended palmarly and the base of the tubercle was made more robust to match the Lesedi specimen. A second reconstruction of U.W. 101-1726 was made with a more extended, ape-like tubercle, with minimal changes to the trapezium-trapezoid facet (Figure S1).

The Tabun C1 scaphoid is missing a small portion from the palmar region of the tubercle. For this specimen, we reconstructed the tubercle in two different ways based on the morphology of the other Neandertal specimens, with one reconstruction

26927691, 2025, 4, Downloaded from https://onlinelibrary.wiley.com/doi/10.1002/ajpa.70157 by NICE, National Institute for Health and Care Excellence, Wiley Online Library on [09/12/2025]. See the Terms and Conditions (https://onlinelibrary.wiley.com/terms-and-conditions) on Wiley Online Library for rules of use; OA articles are governed by the applicable Creative Commons License

having a slightly more robust and more extended tubercle than the other (Figure S2).

2.3 | Data Collection

The morphology of the scaphoid was captured using 10 main anatomical landmarks (detailed in Table 3), 182 curve sliding semi-landmarks and 217 surface sliding semi-landmarks (Figure 3). Curve semilandmarks were selected to outline the articular facets of the scaphoid; however the trapezium and trapezoid facets were grouped together due to difficulty in distinguishing the boundary between these two facets. A boundary tracing the scaphoid waist was selected to encompass the tubercle excluding the dorsal sulcus. The dorsal sulcus was not landmarked due to the natural morphology of the structure, which is porous in nature, and thus not relevant for this analysis of scaphoid shape. Fixed and curve landmarks were placed manually on surface models for each specimen, while surface landmarks were placed on a reference specimen. Landmarking was done in Avizo 6.3, and all landmarks were checked on all specimens by NS and two co-authors (M.M.S. and T.L.K.).

TABLE 3 | Geometric morphometric main anatomical landmark positions. Also see Figure 3.

Landmark	Description
Capitate	0: Dorsal most point on the capitate articular surface bordering the trapezium/trapezoid facet
	1: Palmar most maximum point on the capitate articular surface bordering the trapezium/trapezoid facet
	2: Dorsal most point on the capitate articular surface bordering the lunate facet
	3: Palmar most point on the capitate articular surface bordering the lunate facet
Radius	4: Dorsal most point on the radial articular surface bordering the lunate facet
	5: Palmar most point on the curve of the radial articular facet
Trapezium/Trapezoid	6: Palmar most point on the trapezium/trapezoid articular surface bordering the capitate facet
	7: Dorsal most point on the trapezium/trapezoid articular surface bordering the capitate facet
Tubercle	8: Dorsal most point on the non-articular surface bordering the trapezium/trapezoid facet
	9: Palmar most point on the non-articular surface bordering the lunate and radial facets

2.4 | Shape Variation and Statistical Analyses

GM analyses were carried out in R 4.4.0 (R Core Team 2021) using the packages Morpho 2.1.2 (Schlager 2017), Geomorph 4.0.7 (Adams et al. 2021; Baken et al. 2021) and princurve 2.1.6 (Cannoodt and Bengtsson 2019). A smooth curve was fit through the curve landmark sets using a cubic spline function, and the fixed landmarks were projected on to these curves to divide them into sections. A fixed number of equidistantly spaced landmarks were then placed along each section of these curves (Figure 3). Surface landmarks from the template specimen were then projected on to the remaining sample and relaxed against the template. Curve semi-landmarks were then allowed to slide along tangents to their curves, and surface semilandmarks along tangent planes to the surface, in order to minimize the bending energy of the thin-plate spline interpolation function calculated between each specimen and the Procrustes average for the sample (Gunz and Mitteroecker 2013). The sliding procedure was performed twice, and landmarks were projected back on to their curves/surfaces following each step, after which the semi-landmarks were considered to be geometrically homologous. Next, the landmarks were converted into shape coordinates using generalized least squares Procrustes superimposition, removing the scale, location and orientation information from the coordinates (Gower 1975; Rohlf and Slice 1990; Goodall 1991; Dryden and Mardia 1998).

Principal components analysis (PCA) was carried out in shape space using the package Morpho (Schlager 2017), with the Procrustes coordinates of each specimen. The shape changes were visualized using surface warps generated in R, via Thin-Plate Spline mapping of 3D coordinates saved as a (.tps) file. The analyzed landmarks were then visualized on the surface warps, which show the extremes (1.5 standard deviations) of each PC to understand the shape deformation that occurred. The species means represent the average shape of all specimens within a group, calculated from Procrustes-aligned landmark coordinates and visualized using surface warps. Size differences were calculated using the logarithm of centroid size and subsequently visualized using box-and-whisker plots. Permutational ANOVA tests were carried out solely on the extant sample due to small fossil sample sizes. Permutational tests using 10,000 permutations were done using Procrustes coordinates to assess shape differences using the permudist function after a general Procrustes analysis within the Morpho 2.1.2 package (Adams et al. 2021; Baken et al. 2021; Schlager 2017). To test for allometric effects on shape, we performed a Procrustes ANOVA using residual randomization in a permutation procedure (RRPP) with 10,000 iterations, regressing shape coordinates against centroid size. The analysis was conducted using the ProcDlm function within the geomorph 4.0.7 package. Pairwise comparisons were then carried out using both Procrustes coordinates and centroid size in R, with a Bonferroni post hoc correction shown as comparisons of group variances and distances between group means for Procrustes coordinates, and distances between variances for centroid size. Intraobserver tests were run on both the anatomical landmarks and curve sliding semi-landmarks on three *P. troglodytes* specimens with each landmark being repeated five times with intervals of at least 3 days

26927691, 2025, 4, Downloaded from https://onlinelibrary.wiley.com/doi/10.1002/ajpa.70157 by NICE, National Institute for Health and Care Excellence, Wiley Online Library on [09/12/2025]. See the Terms and Conditions (https://onlinelibrary.wiley.com/terms-and-conditions) on Wiley Online Library for rules of use; OA articles are governed by the applicable Creative Commons License

between each landmarking process. Assessment of intraobserver variation was visualized using a PCA. Interobserver tests were run on the same three *P. troglodytes* specimens, with both the anatomical landmarks and curve sliding semi-landmarks completed by another individual shown in a darker shade on the PCA.

3 | Results

3.1 | Scaphoid Shape and Size Variation in Extant Taxa

All great apes are significantly different ($p < 0.001$) from humans in scaphoid shape, and pairwise comparisons were not significantly different between all taxa except between *G. gorilla, G. beringei* and *P. troglodytes* (Table 4). Potential intraspecific sex differences could not be tested due to small sample sizes or unknown sex in some taxa.

Centroid size explains a small proportion of shape variation (Rsq = 0.0166) and this relationship was not statistically significant (F = 1.23, Z = 0.69, $p = 0.245$). These results suggest that, across the pooled sample, size does not significantly influence shape variation. Statistical pairwise comparisons of centroid sizes across the extant sample indicate that *G. gorilla* is significantly larger than *H. sapiens* and *P. troglodytes* ($p < 0.01$) (Table S3). A box-and-whisker plot of log centroid size depicts the variation in scaphoid size across the extant and fossil samples (Figure 4). Among the fossil hominins, Neandertals have a similar mean centroid size to *H. sapiens*, *A. sediba* and *H. naledi* are the smallest within our sample, and StW 618 is larger than *A. sediba* and *H. naledi*.

3.2 | Inter- and Intraspecific Variation in Landmark Configuration

The intraobserver error test, performed on both anatomical landmarks and curve sliding semi-landmarks, showed clear delineation among the three *P. troglodytes* individuals. Principal component analysis demonstrated that repeated trials clustered tightly within each specimen's convex hull, indicating that the

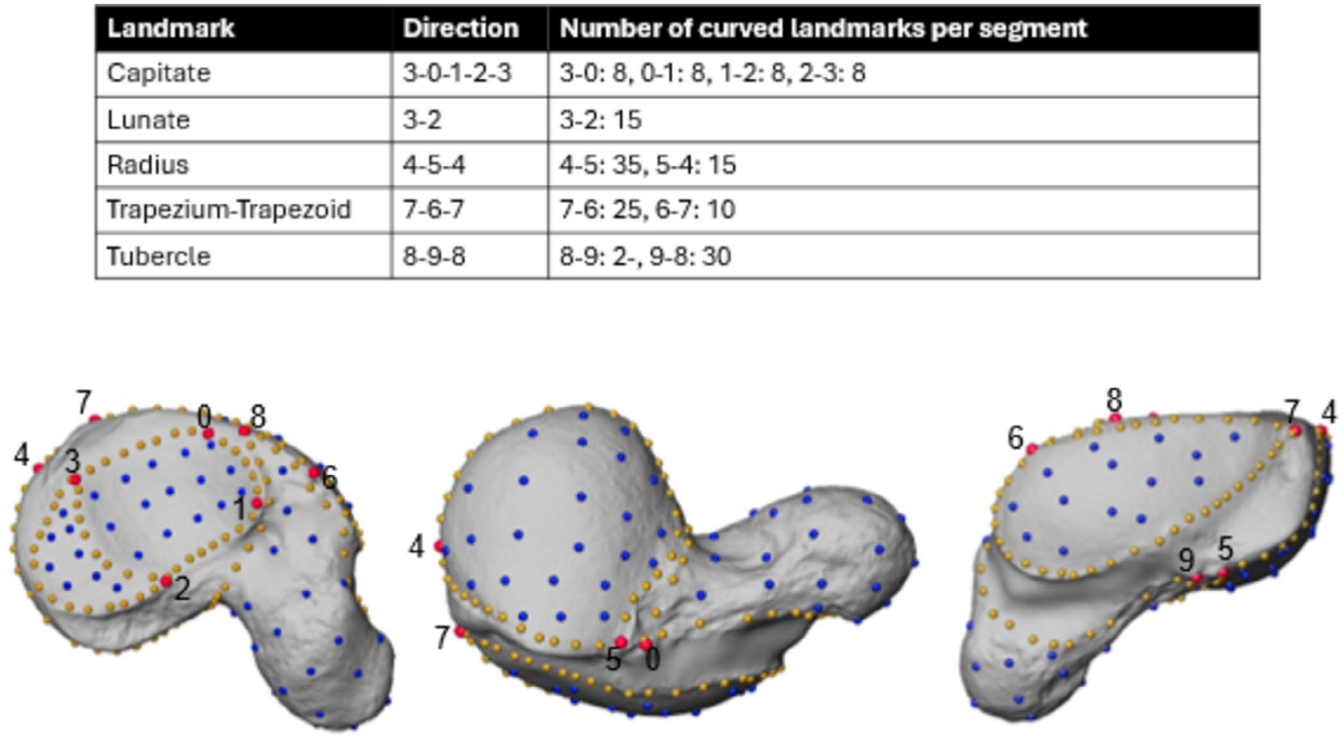

Landmark	Direction	Number of curved landmarks per segment
Capitate	3-0-1-2-3	3-0: 8, 0-1: 8, 1-2: 8, 2-3: 8
Lunate	3-2	3-2: 15
Radius	4-5-4	4-5: 35, 5-4: 15
Trapezium-Trapezoid	7-6-7	7-6: 25, 6-7: 10
Tubercle	8-9-8	8-9: 2-, 9-8: 30

FIGURE 3 | A right sided *Gorilla* surface model with the main (red), curve (yellow) and articular (blue) sliding semi-landmarks configuration annotated in the table indicating the number of landmarks within each curve segment present within the image.

TABLE 4 | Permutation tests for significant differences in scaphoid shape, including distances between means and *p*-values in parentheses.

	G. beringei	*P. troglodytes*	*P. paniscus*	*H. sapiens*
G. gorilla	0.096 (1.00)	0.120 **(0.001)**	0.111 (0.068)	0.131 **(0.001)**
G. beringei		0.153 **(0.001)**	0.149 (0.064)	0.160 **(0.001)**
P. troglodytes	—		0.078 (1.000)	0.161 **(0.001)**
P. paniscus	—	—		0.155 **(0.001)**

Note: Bold indicates $p < 0.05$. Gray-shaded cells indicate comparisons within the same species; no differences were expected in these cases.

26927691, 2025, 4, Downloaded from https://onlinelibrary.wiley.com/doi/10.1002/ajpa.70157 by NICE, National Institute for Health and Care Excellence, Wiley Online Library on [09/12/2025]. See the Terms and Conditions (https://onlinelibrary.wiley.com/terms-and-conditions) on Wiley Online Library for rules of use; OA articles are governed by the applicable Creative Commons License

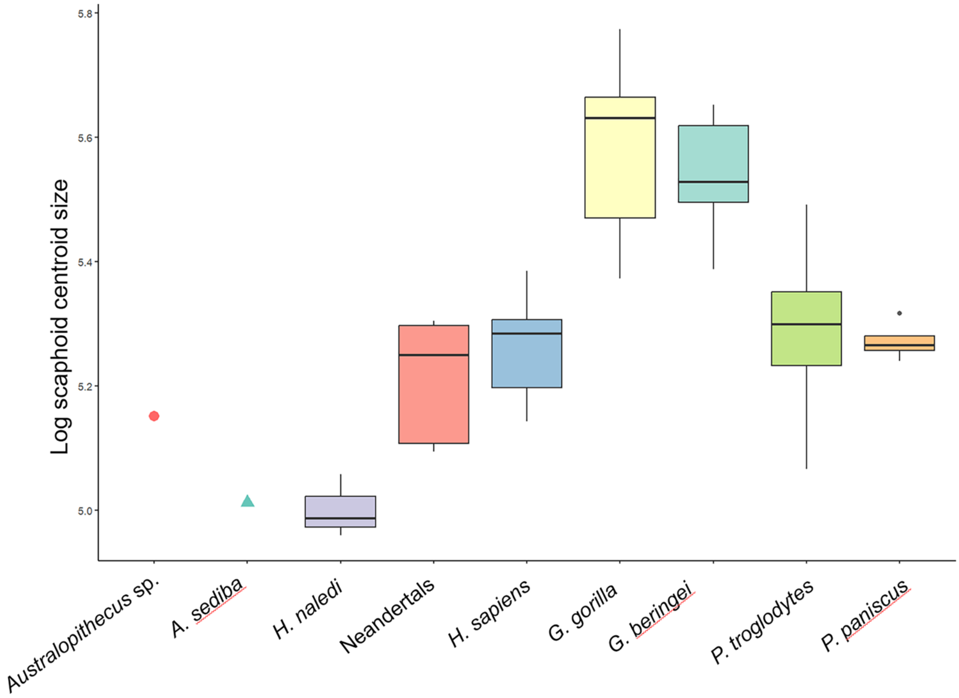

FIGURE 4 | Box-and-Whisker plots indicating centroid size, presented as the logarithm of centroid size, separated by species. Neandertal and *H. naledi* data include all models of their reconstructed morphology.

landmarking protocol was highly repeatable by a single observer (Figure S3). Similarly, the interobserver error test, performed on scaphoid anatomical and curve sliding landmarks on the same three *P. troglodytes* specimens, showed a comparable pattern. The landmarking conducted by a second observer (ST) (Figure S4) clustered closely with the first observer's results, confirming high reproducibility between observers.

3.3 | Analysis of Shape Variation in the Scaphoid

The first three principal components (PCs) account for 40.9% of the variation. In all PCs, the different reconstructed models for *H. naledi* U.W. 101-1726 and Neandertal Tabun C1 fall close to each other. PC1 clearly distinguishes modern humans (apart from one specimen, DCW OC 31 0 1 from Chatham Islands) from African apes, accounting for 17.8% of the variation (Figure 5). Modern humans have an expanded trapezium-trapezoid facet that extends onto the scaphoid tubercle, an open distal border of the capitate facet, a convex, ovoid radial facet, and a thick, short, radially oriented tubercle. The African apes differ from humans in having a long, palmarly oriented tubercle, radiopalmarly oriented trapezium and trapezoid facet, and a flatter radial facet with a scaphoid beak along the distal border. Along PC1, Neandertals cluster with modern humans, whereas *Australopithecus* sp. aligns more closely with *Gorilla*. *A. sediba* and *H. naledi* plot near the modern human range.

The PC2 (14.3%) separates *Pan* from *Gorilla*, as well as *H. sapiens and* Neandertals from *H. naledi* (Figure 5). *Pan*, and particularly *P. troglodytes*, shows a more rectangular capitate facet while *Gorilla* has a circular radial facet with a less pronounced scaphoid beak. *Gorilla*, in particular, is driving the positive extreme axis of PC2, with a long, palmarly oriented tubercle, radiopalmarly oriented trapezium and trapezoid facet, a flatter radial facet with a scaphoid beak along the distal border, and a flatter lunar facet, oriented proximo radially. Neandertals overlap with most modern humans along PC2, but SD 1243 is distinct in having a more rectangular-shaped capitate facet.

The third PC (9.3%) primarily separates both *H. naledi* specimens along the positive axis from the remaining taxa (Figure 5). The *H. naledi* specimens have a broader semilunar-shaped lunate facet that is oriented distopalmarly, alongside a more proximally oriented trapezium-trapezoid facet compared to extant apes. *A. sediba* and Neandertals exhibit a smaller semilunar-shaped lunate facet compared with *H. naledi* and in *A. sediba* this facet is oriented more distopalmarly than that of Neandertals. The humans and extant apes are separated along the negative axis of this PC. A summary of the distinguishing morphological features for each taxon is presented in Figures 6–8.

4 | Discussion

This study quantified extant African ape, *H. sapiens* and extinct hominin scaphoid shape using 3D landmark-based GM to comprehensively analyze inter- and intraspecific shape variation, and how it may relate to differences in locomotor and manipulative behaviors. Given the complexity of scaphoid shape, this proof-of-concept study predicted that 3D GM would provide better discrimination in scaphoid morphology across extant taxa compared with previous studies (e.g., Kibii et al. 2011; Kivell, Churchill, et al. 2018; Kivell, Rosas, et al. 2018; Kivell and Begun 2009; Tocheri et al. 2007), which was supported by our results. Our expectations of how each fossil hominin scaphoid would compare morphologically to extant taxa based

26927691, 2025, 4, Downloaded from https://onlinelibrary.wiley.com/doi/10.1002/ajpa.70157 by NICE, National Institute for Health and Care Excellence, Wiley Online Library on [09/12/2025]. See the Terms and Conditions (https://onlinelibrary.wiley.com/terms-and-conditions) on Wiley Online Library for rules of use; OA articles are governed by the applicable Creative Commons License

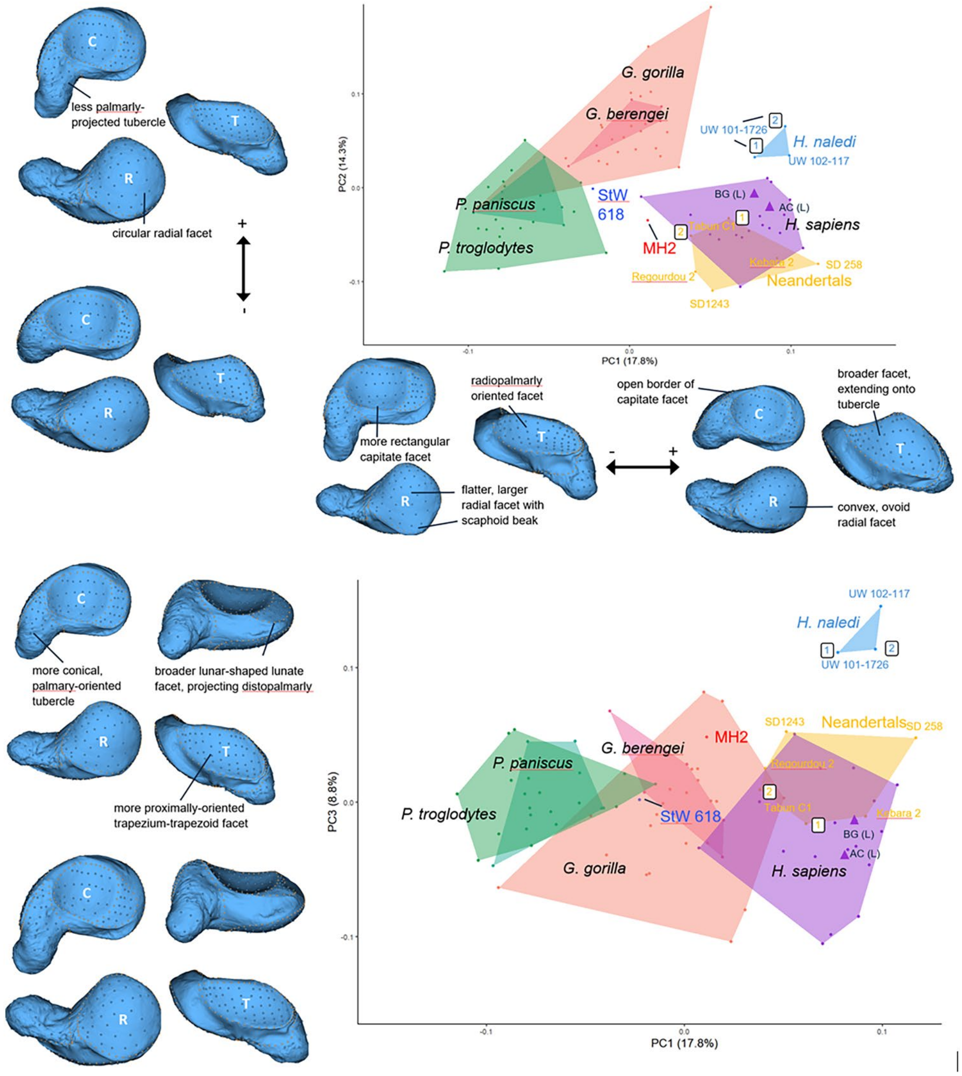

FIGURE 5 | Principal component analysis of scaphoid shape. Results of PC1 versus PC2 (A) and PC1 versus PC3 (B). All results of the PCAs are shown with associated shape changes. Articular facets are labeled for capitate (C), lunate (L), radius (R) and trapezium-trapezoid (T). Multiple data points for Tabun C1 and *H. naledi* U.W. 101-1726 represent different reconstructed morphologies (see Figures S1 and S2).

on previous morphological descriptions, however, were not always supported. We discuss these results in more detail below.

4.1 | Scaphoid Shape Variation and Function in Extant Hominines

The morphological differences that separate humans and African apes are consistent with the many previous qualitative and quantitative studies of scaphoid hominine morphology (e.g., Begun 2004; Kivell and Schmitt 2009; Kibii et al. 2011; Kivell 2016). For example, African apes typically share a long, palmarly-oriented tubercle, radiopalmarly-oriented trapezium-trapezoid facet, and a flatter radial facet with a scaphoid beak, the latter which is more prominent in *Pan* than in *Gorilla*. This morphology is consistent with frequent compressive loads sustained during knuckle-walking (Marzke 1971; Begun 2004; Hamrick 1997; Sarmiento 1988; Püschel et al. 2020) as well as a deep carpal tunnel that accommodates well-developed wrist and digit flexor muscles for arboreal and manipulative behaviors (Taverne et al. 2018; R. H. Tuttle 1969).

We also found some discrimination in scaphoid morphology between *Gorilla* and *Pan*. *Gorilla* shows a more circular capitate facet, a larger, more circular radial facet and a less pronounced scaphoid beak compared with *Pan* (Kivell and Schmitt 2009). Within *Pan*, *P. troglodytes* typically has a more ovoid-shaped capitate facet and a more square-shaped lunate facet than *P. paniscus*. In contrast, *P. paniscus* typically has a diamond-shaped radial facet (i.e., proximodistally longer than it is radioulnarly wide) and is more similar to *Gorilla* in having a shallower, circular capitate facet and palmarly oriented tubercle (see also Kivell 2007).

The slight differences in scaphoid morphology across African apes may reflect differences in hand use during locomotion. *Pan* is considered to use more variable hand postures than *Gorilla* (D. M. Doran 1993; van Lawick-Goodall 1968; Crompton et al. 2010; D. M. Doran 1996; Inouye 1994; H. Tuttle 1985; Wunderlich and Jungers 2009), while *P. paniscus* has been shown to use more palmigrade postures in the trees than *P. troglodytes* (D. M. Doran 1993). However, studies of hand posture, particularly in an arboreal environment and in wild populations are limited,

26927691, 2025, 4, Downloaded from https://onlinelibrary.wiley.com/doi/10.1002/ajpa.70157 by NICE, National Institute for Health and Care Excellence, Wiley Online Library on [09/12/2025]. See the Terms and Conditions (https://onlinelibrary.wiley.com/terms-and-conditions) on Wiley Online Library for rules of use; OA articles are governed by the applicable Creative Commons License

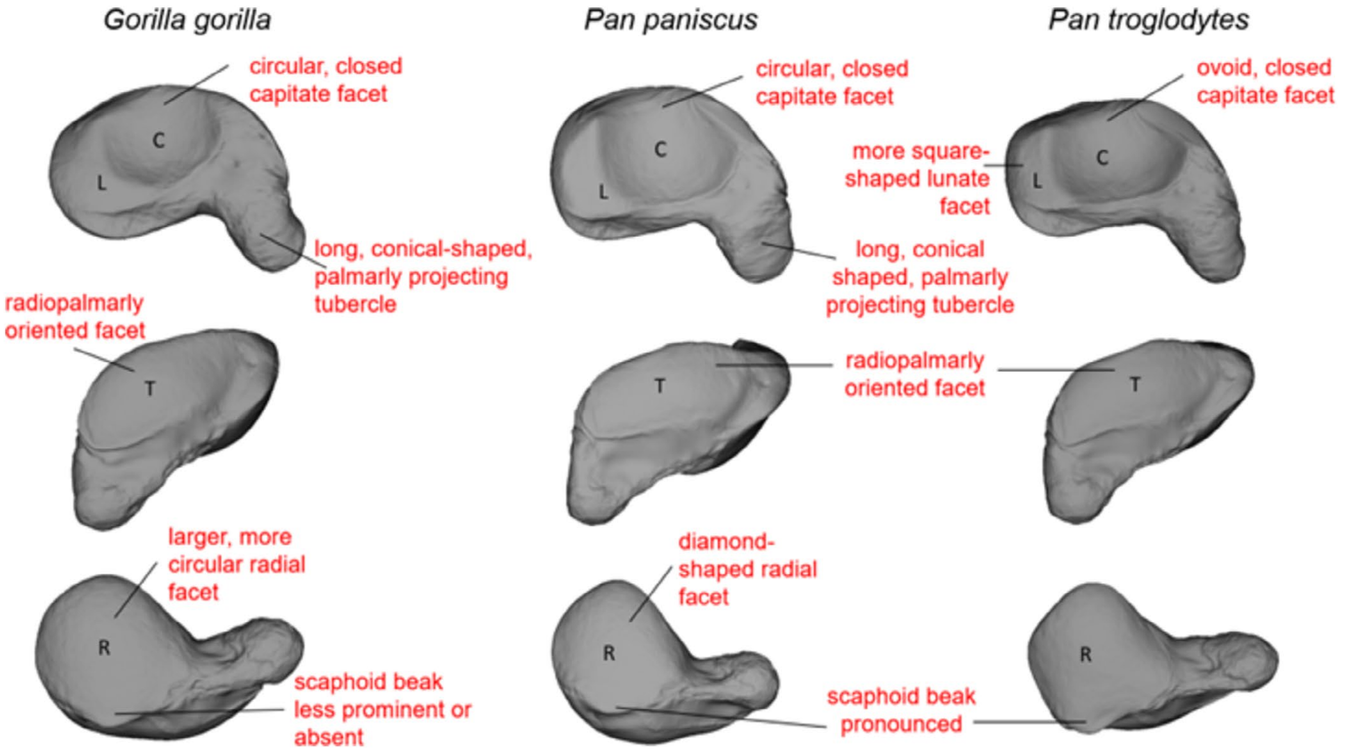

FIGURE 6 | Scaphoid mean species surface model images of extant African apes with key morphological features highlighted. African ape (or ape-like) features are in red text. All images are shown in distal (top), proximal (middle) and dorsal (bottom) views and visualized on mean models for extant taxa. Articular facets are labeled for capitate (C), lunate (L), radius (R) and trapezium-trapezoid (T) for right-sided specimens.

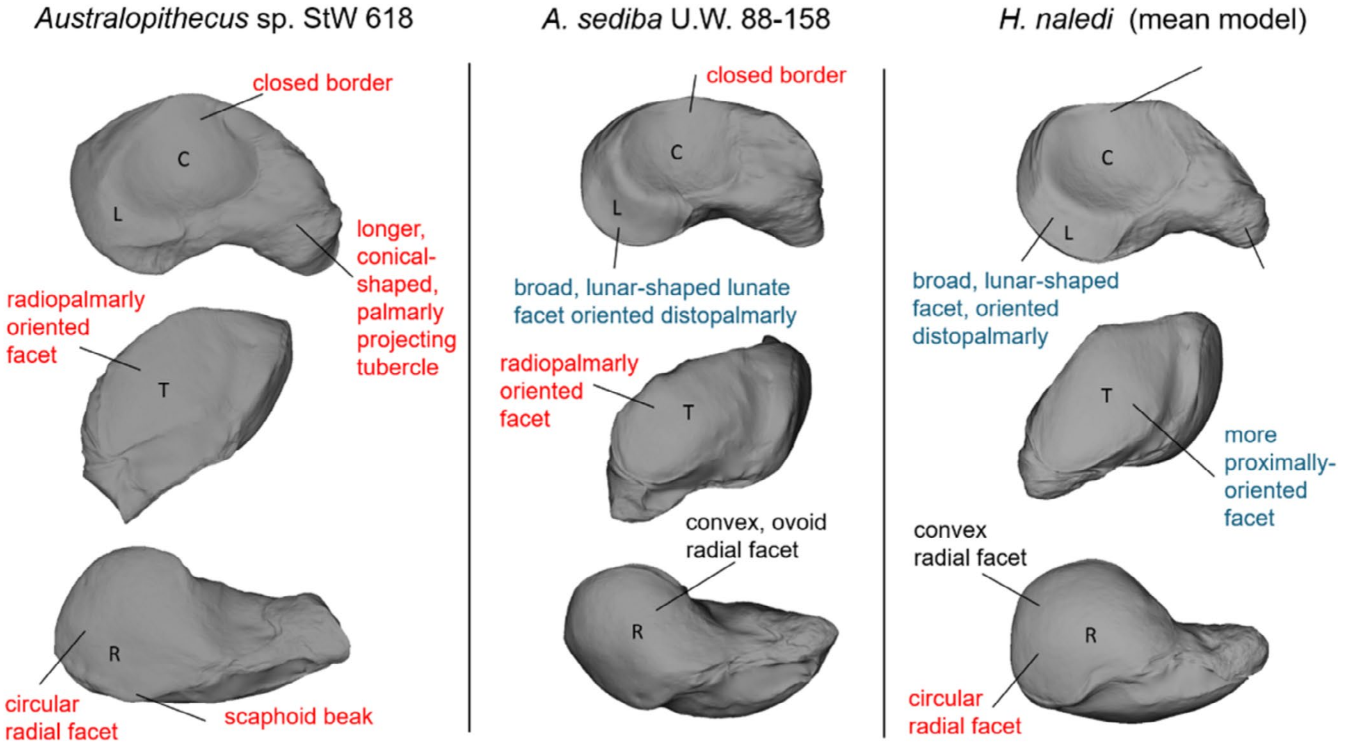

FIGURE 7 | Scaphoid mean species surface model images of South African hominins with key morphological features highlighted. African ape (or ape-like) features are in red text, human (or human-like) features in black text, and distinct features are in blue text. All images are shown in distal (top), proximal (middle) and dorsal (bottom) views and visualized on mean models for *H. naledi*. Articular facets are labeled for capitate (C), lunate (L), radius (R) and trapezium-trapezoid (T) for right-sided specimens.

26927691, 2025, 4, Downloaded from https://onlinelibrary.wiley.com/doi/10.1002/ajpa.70157 by NICE, National Institute for Health and Care Excellence, Wiley Online Library on [09/12/2025]. See the Terms and Conditions (https://onlinelibrary.wiley.com/terms-and-conditions) on Wiley Online Library for rules of use; OA articles are governed by the applicable Creative Commons License

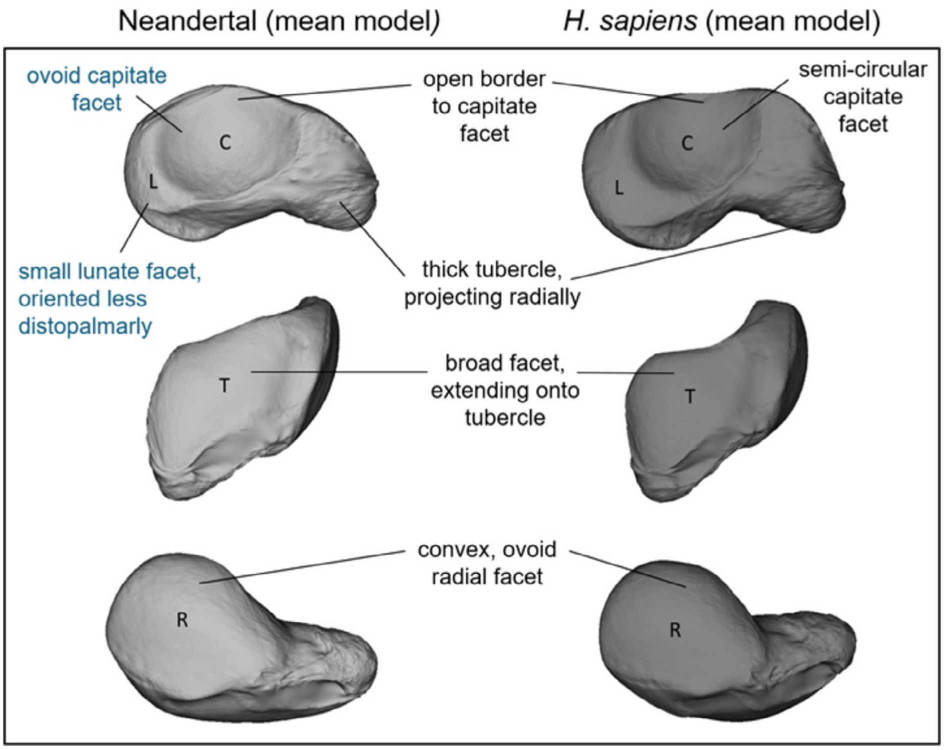

FIGURE 8 | Scaphoid mean species surface model images of Neandertal and *H. sapiens* (with key morphological features highlighted. Human (or human-like) features in black text, and distinct features are in blue text). All images are shown in distal (top), proximal (middle) and dorsal (bottom) views and visualized on mean models for *H. sapiens* and Neandertals. Articular facets are labeled for capitate (C), lunate (L), radius (R) and trapezium-trapezoid (T) for right-sided specimens.

especially in *P. paniscus*. Thompson (2020) suggests that the more prominent scaphoid beak could be due to the increased frequency of arboreal locomotion in *Pan*, relative to *Gorilla*, rather than being an adaptation solely for knuckle-walking. More information is needed on positional behavior and hand use in wild *Pan* populations to understand if slight differences in scaphoid morphology are functionally significant or are part of a suite of morphological features that differ between *P. paniscus* and *P. troglodytes* (Zihlman and Cramer 1978; Zihlman 1984) but do not necessarily reflect functional (kinematic) differences (Druelle et al. 2018).

In zoo-settings, *Gorilla* has been shown to use less variable hand postures relative to *Pan*, and have more equal metacarpal lengths that allow for a more even distribution of force across the metacarpals during terrestrial knuckle-walking than in *Pan* (Inouye 1994; Matarazzo 2013). In addition, wild *Gorilla* are thought to engage in lower frequencies of arboreal locomotion than *Pan*. Together these locomotor and postural differences may be reflected in the *Gorilla* scaphoid morphology. Kivell and Schmitt (2009) hypothesized that the limited development of a scaphoid beak in *Gorilla*, as well as other carpal features typically associated with limiting extension during knuckle-walking, may reflect a more columnar wrist and forelimb posture in *Gorilla* compared with *Pan*, in which bony adaptations for limiting wrist extension are not necessary. However, more recent kinematic analyses of zoo-living animals show similarity in African ape wrist and forelimb kinematics during terrestrial knuckle-walking (Finestone et al. 2018) and that *Gorilla* use a more, rather than less, extended wrist posture during arboreal knuckle-walking (Tarrega-Saunders et al. 2021). Furthermore, Thompson et al. (2018) documented wild mountain gorillas (*G. beringei*) utilizing a variety of hand postures on the ground, including fist-walking, modified palmigrady and dorsal-metacarpal weightbearing postures, in addition to knuckle-walking. It is also important to note that the degree of arboreality in *Gorilla* has previously been quantified in one population of *G. beringei* from the Virunga mountains, Rwanda (D. M. Doran 1996, 1997). Recently, Robbins et al. (2025) showed that both *G. gorilla* (from Loango National Park, Gabon) and a different population of *G. beringei* (from Bwindi Impenetrable National Park, Uganda) are more arboreal than previously thought. With adult females and males spending between 18% and 34% of their time in the trees, gorillas show levels of arboreality approaching that of male chimpanzees (Robbins et al. 2025). However, given the small sample sizes in the present study, we found minimal distinction between the two gorilla species.

The human-like features revealed by our analysis include an expanded trapezium-trapezoid facet that extends onto the tubercle, an open distal border of the capitate facet, a convex, ovoid-shaped radial facet, and a stout, radially oriented tubercle. These morphological features of the human scaphoid have been highlighted in previous comparative studies of hominoid scaphoid (e.g., Kibii et al. 2011; Kivell 2016; Kivell, Churchill, et al. 2018; Kivell, Rosas, et al. 2018; Tocheri 2007; Tocheri et al. 2008). For example, the expanded trapezium-trapezoid facet and open capitate facet reflect changes in the trapezoid shape and the more supinated orientation of the trapezium that together are thought to help withstand high radioulnarly directed loads from the

26927691, 2025, 4, Downloaded from https://onlinelibrary.wiley.com/doi/10.1002/ajpa.70157 by NICE, National Institute for Health and Care Excellence, Wiley Online Library on [09/12/2025]. See the Terms and Conditions (https://onlinelibrary.wiley.com/terms-and-conditions) on Wiley Online Library for rules of use; OA articles are governed by the applicable Creative Commons License

thumb (Tocheri 2007). The convex radial facet may facilitate the higher range of wrist extension found in humans relative to African apes (R. H. Tuttle 1969), which has been shown to provide a mechanical advantage when using the dart thrower's motion (Rohde et al. 2010; Wolfe et al. 2006). Our two fossil *H. sapiens* specimens—Arene Candide 2 and Barma Grande 2—fell out within our recent *H. sapiens* distribution, indicating a similar morphology.

4.2 | Scaphoid Shape Variation in Fossil Hominins

Our comparative analysis revealed that each fossil hominin taxon occupied a distinct position within the PCA morphospace, indicating a unique suite of features that could suggest differing capabilities of locomotion and manipulation. We discuss the functional morphology of each fossil taxon below.

As predicted, our Neandertal sample showed many morphological similarities to *H. sapiens*; a result that has been recognized by several previous studies (e.g., Trinkaus 1983; Tocheri 2007; Tocheri et al. 2008) and reflects their shared derived morphology that first appeared in the fossil hominin record by at least 0.8 Ma (Lorenzo et al. 1999; Tocheri et al. 2008; Kivell, Churchill, et al. 2018; Kivell, Rosas, et al. 2018; Orr et al. 2013). However, some of our Neandertal sample fell out in separate morphospace, next to *H. sapiens*, reflecting some differences in scaphoid morphology that make Neandertals distinct. These features were a smaller lunate facet, that is oriented less distopalmarly than in *H. sapiens* and a more ovoid capitate facet. The El Sidrón specimens share a trapezium facet that expands almost to the tip of the extremely robust scaphoid tubercle, but SD 1243 has a flatter dorsal portion of the trapezium-trapezoid facet while SD 258 is distinct in preserving a 'os centrale' portion along the distal border of its capitate facet (Kivell, Churchill, et al. 2018; Kivell, Rosas, et al. 2018). The Kebara 2 specimen has a radioulnarly expanded dorsal portion of the trapezium-trapezoid facet that more closely resembles that of *H. sapiens* and distinguishes it from all other Neandertal specimens in our sample.

Both Neandertals and early *H. sapiens* have been found in association with similar Middle Paleolithic (Mousterian) tool technologies, but subtle differences in hand morphology between these two taxa have been interpreted as reflecting differences in habitual grip use (e.g., Churchill 2001; Bardo et al. 2020; Niewoehner 2001; Niewoehner et al. 1997; Trinkaus 1983). In particular, robust phalanges, hypertrophied muscle attachments, a more parasagittally oriented capitate-second metacarpal articulation, reduced third metacarpal styloid process, and large, projecting carpal tubercles have been interpreted as evidence that power grips were more frequently used by Neandertals compared to contemporaneous *H. sapiens* (Churchill 2001; Niewoehner 2001; Niewoehner 2006; Trinkaus 1983). Moreover, the distinct articular facet shapes and orientations between the trapezium and first and second metacarpals in Neandertals suggest frequent use of extended and adducted thumb postures, such as grips commonly used for hafted tools (Bardo et al. 2020). Although Neandertal hand morphology is also consistent with habitual use of precision grips (Feix et al. 2015; Karakostis et al. 2018), differences we find between Neandertal and *H. sapiens* scaphoid morphology are consistent with subtle differences in habitual thumb posture and loading.

The *Australopithecus* sp. StW 618 specimen plots near or within the *Gorilla* distribution in the first three principal components. This result is consistent with our predictions and the original description of this fossil in being more African ape-like than human-like (Kibii et al. 2011). This fossil shares with *Gorilla* circular capitate and radial facets, the presence of a slight scaphoid beak and a long, conical-shaped and palmarly projecting tubercle. This morphology indicates a scaphoid that does not necessarily preclude dextrous manipulation, though possibly in a less efficient manner compared with later hominins (Kibii et al. 2011; Marzke and Marzke 2000). Most of the hominin material recovered from the Member 4 deposits has been attributed to *Australopithecus africanus* (Kibii et al. 2011) but other australopith species may be present at Sterkfontein (Clarke 1994; Lockwood and Tobias 2002; Crompton et al. 2021). The upper limb of other *A. africanus* specimens shows morphology that would facilitate arboreal locomotion, such as a superiorly oriented glenoid fossae (Susan G. Larson 2009; Vrba 1979) and low humeral torsion (S. G. Larson 1996) in this bipedal hominin.

A. sediba MH2 scaphoid plots between African apes and humans in our comparative analysis. This result reflects its mix of ape-like features, such as a radiopalmarly-oriented trapezium-trapezoid facet, a more closed distal border of the capitate facet, a human-like radial facet, and intermediate features, such as a smaller tubercle compared to that of extant apes but that is less radially projecting than that of humans. Together this morphology suggests the loading of the scaphoid during both locomotion and manipulation, in which the latter may have been at a greater frequency and/or dextrous ability than earlier australopiths (e.g., StW 618) but less than later *Homo*. Although *A. sediba* has not yet been found in association with tools (Berger et al. 2010), its thumb length is longer than that of modern humans, suggesting pad-to-pad precision grasping was possible (Kivell et al. 2011; Kivell, Churchill, et al. 2018; Kivell, Rosas, et al. 2018; Bardo et al. 2018). The associated MH2 upper limb shows several ape-like features consistent with climbing behaviors, such as cranially-oriented glenoid fossa and scapular spine, increased attachment area for the supraspinatus muscle on the scapula, low humeral torsion and an increased brachial index (Churchill et al. 2013). The internal bone structure of the MH2 metacarpals also indicates a mosaic pattern of both locomotor and manipulative behaviors, suggesting orangutan-like grasping by the fingers and human-like loading of the thumb (Dunmore et al. 2020).

Our analysis shows that the *H. naledi* scaphoids share with *Gorilla* more circular radial and capitate facets and an elongated, conical-shaped tubercle that projects more palmarly compared to humans and Neandertals. These *Gorilla*-like features may reflect habitual climbing in *H. naledi*, as suggested by the well-developed longitudinal curvature (Kivell et al. 2015) and cortical bone distribution of the manual phalanges (Syeda et al. 2025) and ape-like features of the upper limb (Feuerriegel et al. 2017, 2019). The *H. naledi* scaphoids also exhibit a human-like, strongly convex radial facet, which is consistent with other human-like features of the Hand 1 carpus, such as a robust first metacarpal and human-like hand proportions (Kivell et al. 2015).

26927691, 2025, 4, Downloaded from https://onlinelibrary.wiley.com/doi/10.1002/ajpa.70157 by NICE, National Institute for Health and Care Excellence, Wiley Online Library on [09/12/2025]. See the Terms and Conditions (https://onlinelibrary.wiley.com/terms-and-conditions) on Wiley Online Library for rules of use; OA articles are governed by the applicable Creative Commons License

4.3 | Limitations

This study applies geometric morphometric techniques to a sample comprising both extant and fossil specimens spanning a range of geographical and temporal contexts. While the landmark-based approach provides high-resolution shape data, the sample sizes in our study are a limiting factor. Small sample sizes can restrict the statistical power of multivariate analyses, increase the influence of individual variation, and limit the generalizability of observed patterns (Cardini et al. 2015). In addition, sample imbalance restricted our ability to assess sex-based shape variation, meaning that sexual dimorphism may contribute to some of the observed differences. To mitigate these effects, landmark configurations were carefully standardized, specimens with incomplete or poorly preserved morphology were excluded, and reconstructions were performed using validated comparative methods where necessary. Nonetheless, all results should be interpreted with caution, and future studies incorporating larger, sex-balanced samples will be essential for testing the robustness of the morphological trends identified here, alongside the inclusion of other fossil scaphoid samples such as that of *Ardipithecus ramidus* (Lovejoy et al. 2009) and Middle Pleistocene *Homo* from Sima de los Huesos (Sala et al. 2024).

5 | Conclusion

Shape is an important component of carpal function, as it dictates stability and range of motion. The use of 3D GM to quantify scaphoid shape allows for a whole bone approach that better captures shape (and size) variation across extant hominines, including subtle differences between *Gorilla* and *Pan* and within *Pan*, than has been demonstrated previously by other 3D (Tocheri et al. 2007) and 2D methods (Kivell and Begun 2009; Kivell et al. 2011). Our analysis also highlights morphological differences between Neandertal and *H. sapiens*, and distinct morphologies of the scaphoid in all three South African fossil hominins. In contrast to previous studies (Kivell et al. 2011, 2015; Kivell, Churchill, et al. 2018; Kivell, Rosas, et al. 2018), our analysis suggests that *A. sediba*, at 1.98 Ma (Pickering et al. 2011), has more human-like scaphoid morphology than *H. naledi*, at ~300 Ka (Robbins et al. 2021). The functional significance, if any, of this difference, as well as subtle variation between some extant (e.g., *P. paniscus* and *P. troglodytes*) and fossil taxa (e.g., Neandertals and *H. sapiens*), remains unclear and should be considered within the context of articulating hand bones and overall morphology of the carpus. Our study demonstrates the value of using 3D GM to quantify the complex morphology of the scaphoid that can be applied to other carpal (and tarsal) bones to reveal morphological variation between closely related taxa.

Author Contributions

Nadine G. Steer: conceptualization (equal), formal analysis (lead), funding acquisition (supporting), investigation (lead), methodology (equal), project administration (lead), visualization (lead), writing – original draft (lead), writing – review and editing (equal). **Ameline Bardo:** formal analysis (equal), investigation (equal), methodology (equal), visualization (equal), writing – review and editing (equal). **Thomas W. Davies:** conceptualization (equal), formal analysis (supporting), investigation (equal), methodology (equal), resources (equal), visualization (supporting), writing – review and editing (equal). **Antonio Rosas:** data curation (supporting), resources (supporting), writing – review and editing (supporting). **Matthew M. Skinner:** conceptualization (equal), data curation (equal), formal analysis (equal), funding acquisition (lead), investigation (equal), methodology (equal), project administration (equal), resources (equal), software (lead), supervision (equal), validation (equal), visualization (equal), writing – original draft (supporting), writing – review and editing (equal). **Tracy L. Kivell:** conceptualization (lead), data curation (lead), formal analysis (equal), investigation (lead), methodology (equal), project administration (equal), resources (equal), supervision (lead), validation (lead), visualization (equal), writing – original draft (supporting), writing – review and editing (lead).

Acknowledgments

For access to specimens we thank the following individuals/institutions: Max Planck Institute for Evolutionary Anthropology (C. Boesch, J-J. Hublin); Museum für Naturkunde—Leibniz Institute for Evolution and Biodiversity Science (Frieder Mayer and Christiane Funk); Powell-Cotton Museum (I. Livne); Royal Museum for Central Africa (E. Gilissen); University of Florence (J. Moggi-Cecchi, S. Bortoluzzi); Johann-Friedrich-Blumenback-Institute for Zoology and Anthropology, Georg-August University, Goettingen (B. Grosskopf); University of the Witswatersand (L. Berger, B. Zipfel), Museo Nazionale Preistorico dei Balzi Rossi (E. Starnini), Museo Archeologico del Finale (A. De Pascale), Sackler School of Medicine, Tel Aviv University (A. Barash, Y. Rak; I. Herskovitz), National Museum of Natural History in Paris (M. Friess, V. Laborde, L. Huet, A. Fort), and the Duckworth Collection at the University of Cambridge (T. Biers and M. Mirazon Lahr). We thank M. Tocheri for sharing the surface scan of Le Régourdou 1. We would like to thank L. Hunter who provided the scans from the Field Museum of Natural History, American Museum of Natural History and the National Museum of Natural History, Smithsonian Institution, Washington D.C. This project has received funding from the European Research Council (ERC) under the European Union's Horizon 2020 research and innovation programme (grant agreement No. 819960) and the GREAT Scholarship funded by the British Council and University of Kent (NGS). This work was partially funded by the Spanish Ministry of Science and Innovation through the projects PID2021-122356NB-I00 to A.R. Finally, we thank Caley Orr, one anonymous reviewer and the editorial board for their constructive feedback that improved this manuscript.

Data Availability Statement

R data files and code included in this analysis as well as surface models for some specimens are available on https://human-fossil-record.org/. For other specimens that are not freely open access, approval from the respective curatorial institution is required prior to sharing of surface model data.

References

Abrams, G., T. Devièse, S. Pirson, et al. 2024. “Investigating the Co-Occurrence of Neanderthals and Modern Humans in Belgium Through Direct Radiocarbon Dating of Bone Implements.” *Journal of Human Evolution* 186: 103471.

Adams, D., M. Collyer, A. Kaliontzopoulou, and E. Baken. 2021. “Geomorph: Software for Geometric Morphometric Analyses”. https://cran.r-project.org/package=geomorph.

Aranguren, B., A. Revedin, N. Amico, et al. 2018. “Wooden Tools and Fire Technology in the Early Neanderthal Site of Poggetti Vecchi (Italy).” *Proceedings of the National Academy of Sciences* 115, no. 9: 2054–2059.

Arrighi, S., A. Moroni, L. Tassoni, et al. 2020. “Bone Tools, Ornaments and Other Unusual Objects During the Middle to Upper Palaeolithic Transition in Italy.” *Quaternary International* 551: 169–187.

26927691, 2025, 4, Downloaded from https://onlinelibrary.wiley.com/doi/10.1002/ajpa.70157 by NICE, National Institute for Health and Care Excellence, Wiley Online Library on [09/12/2025]. See the Terms and Conditions (https://onlinelibrary.wiley.com/terms-and-conditions) on Wiley Online Library for rules of use; OA articles are governed by the applicable Creative Commons License

Baken, E., M. Collyer, A. Kaliontzopoulou, and D. Adams. 2021. "GmShiny and Geomorph v4.0: New Graphical Interface and Enhanced Analytics for a Comprehensive Morphometric Experience".

Bardo, A., R. Cornette, A. Borel, and E. Pouydebat. 2017. "Manual Function and Performance in Humans, Gorillas, and Orangutans During the Same Tool Use Task." *American Journal of Physical Anthropology* 164, no. 4: 821–836. https://doi.org/10.1002/ajpa.23323.

Bardo, A., M. H. Moncel, C. J. Dunmore, T. L. Kivell, E. Pouydebat, and R. Cornette. 2020. "The Implications of Thumb Movements for Neanderthal and Modern Human Manipulation." *Scientific Reports* 10, no. 1: 1–12. https://doi.org/10.1038/s41598-020-75694-2.

Bardo, A., L. Vigouroux, T. L. Kivell, and E. Pouydebat. 2018. "The Impact of Hand Proportions on Tool Grip Abilities in Humans, Great Apes and Fossil Hominins: A Biomechanical Analysis Using Musculoskeletal Simulation." *Journal of Human Evolution* 125: 106–121.

Begun, D. R. 2004. "Knuckle-Walking and the Origin of Human Bipedalism." In *From Biped to Strider*, edited by D. J. Meldrum and C. E. Hilton, 9–33. Springer. https://doi.org/10.1007/978-1-4419-8965-9_2.

Berger, L. R., D. J. de Ruiter, S. E. Churchill, et al. 2010. "Australopithecus Sediba: A New Species of Homo-Like Australopith From South Africa." *Science* 328, no. 5975: 195–204. https://doi.org/10.1126/SCIENCE.1184944.

Berger, R. A. 1997. "The Ligaments of the Wrist." *Hand Clinics* 13, no. 1: 63–82. https://doi.org/10.1016/s0749-0712(21)00081-0.

Boesch, C., and H. Boesch. 1990. "Tool Use and Tool Making in Wild Chimpanzees." *Folia Primatologica* 54, no. 1–2: 86–99. https://doi.org/10.1159/000156428.

Bowland, L., J. E. Scott, T. L. Kivell, B. A. Patel, M. W. Tocheri, and C. M. Orr. 2021. "Homo Naledi Pollical Metacarpal Shaft Morphology Is Distinctive and Intermediate Between That of Australopiths and Other Members of the Genus *Homo*." *Journal of Human Evolution* 158: 103048.

Cannoodt, R., and H. Bengtsson. 2019. "Rcannood/Princurve: Princurve 2.1.4". https://doi.org/10.5281/zenodo.3351282.

Cardini, A., K. Seetah, and G. Barker. 2015. "How Many Specimens Do I Need? Sampling Error in Geometric Morphometrics: Testing the Sensitivity of Means and Variances in Simple Randomized Selection Experiments." *Zoomorphology* 134: 149–163. https://doi.org/10.1007/s00435-015-0253-z.

Ceri, N., E. Korman, I. Gunal, and S. Tetik. 2004. "The Morphological and Morphometric Features of the Scaphoid." *Journal of Hand Surgery* 29, no. 4: 393–398.

Christel, M. 1993. "Grasping Techniques and Hand Preferences in Hominoidea." In *Hands of Primates*, 91–108. https://doi.org/10.1007/978-3-7091-6914-8_7.

Churchill, S. E. 2001. "Hand Morphology, Manipulation, and Tool Use in Neandertals and Early Modern Humans of the Near East." *Proceedings of the National Academy of Science* 98, no. 6: 2953–2955.

Churchill, S. E., and V. Formicola. 1997. "A Case of Marked Bilateral Asymmetry in the Upper Limbs of an Upper Palaeolithic Male From Barma Grande (Liguria), Italy." *International Journal of Osteoarchaeology* 7: 17–38. https://doi.org/10.1002/(SICI)1099-1212(199701)7:1<18::AID-OA303>3.0.CO;2-R.

Churchill, S. E., T. W. Holliday, K. J. Carlson, et al. 2013. "The Upper Limb of *Australopithecus Sediba*." *Science* 340, no. 6129: 1233477. https://doi.org/10.1126/science.1233477.

Cignoni, P., M. Callieri, M. Corsini, M. Dellepiane, F. Ganovelli, and G. Ranzuglia. 2008. "MeshLab: An Open-Source Mesh Processing Tool. Sixth Eurographics Italian Chapter Conference, 129–136".

Clarke, R. J. 1994. "On Some New Interpretations of Sterkfontein Stratigraphy." *South African Journal of Science* 90: 211–214. https://doi.org/10.10520/AJA00382353_5382.

Corruccini, R. S. 1978. "Comparative Osteometrics of the Hominoid Wrist Joint, With Special Reference to Knuckle-Walking." *Journal of Human Evolution* 7, no. 4: 307–321. https://doi.org/10.1016/S0047-2484(78)80072-4.

Crompton, R. H., J. McClymont, S. Elton, et al. 2021. "StW 573 Australopithecus Prometheus: Its Significance for an Australopith Bauplan." *Folia Primatologica* 92, no. 5–6: 243–275. https://doi.org/10.1159/000519723.

Crompton, R. H., J. McClymont, S. Thorpe, et al. 2018. "Functional Anatomy, Biomechanical Performance Capabilities and Potential Niche of StW 573: An *Australopithecus* Skeleton (Circa 3.67 ma) From Sterkfontein Member 2, and Its Significance for the Last Common Ancestor of the African Apes and for Hominin Origins. *BIoRxiv*, 481556".

Crompton, R. H., W. I. Sellers, and S. K. S. Thorpe. 2010. "Arboreality, Terrestriality and Bipedalism." *Philosophical Transactions of the Royal Society B: Biological Sciences* 365, no. 1556: 3301–3314. https://doi.org/10.1098/RSTB.2010.0035.

Delpech, F. 1996. "L'environnement Animal Des Moustériens Quina du Périgord." *Paléo* 8, no. 1: 31–46.

Dirks, P. H. G. M., E. M. Roberts, H. Hilbert-Wolf, et al. 2017. "The Age of Homo Naledi and Associated Sediments in the Rising Star Cave, South Africa." *ELife* 6. https://doi.org/10.7554/ELIFE.24231.

Doran, D. M. 1993. "Comparative Locomotor Behavior of Chimpanzees and Bonobos: The Influence of Morphology on Locomotion." *American Journal of Physical Anthropology* 91, no. 1: 83–98. https://doi.org/10.1002/ajpa.1330910106.

Doran, D. M. 1996. "Comparative Positional Behavior of the African Apes." In *Great Ape Societies*, 213–224. Cambridge University Press. https://ci.nii.ac.jp/naid/10010164749.

Doran, D. M. 1997. "Ontogeny of Locomotion in Mountain Gorillas and Chimpanzees." *Journal of Human Evolution* 32, no. 4: 323–344.

Druelle, F., K. Schoonaert, P. Aerts, S. Nauwelaerts, J. M. G. Stevens, and K. D'Août. 2018. "Segmental Morphometrics of Bonobos (*Pan paniscus*): Are They Really Different From Chimpanzees (*Pan troglodytes*)?" *Journal of Anatomy* 233: 843–853. https://doi.org/10.1111/joa.12894.

Drummond-Clarke, R. C., T. L. Kivell, L. Sarringhaus, F. A. Stewart, T. Humle, and A. K. Piel. 2022. "Wild Chimpanzee Behavior Suggests That a Savanna-Mosaic Habitat Did Not Support the Emergence of Hominin Terrestrial Bipedalism." *Science Advances* 8, no. 50: eadd9752. https://doi.org/10.1126/sciadv.add9752.

Drummond-Clarke, R. C., T. L. Kivell, L. Sarringhaus, F. A. Stewart, and A. K. Piel. 2024. "Sex Differences in Positional Behavior of Chimpanzees (*Pan troglodytes schweinfurthii*) Living in the Dry and Open Habitat of Issa Valley, Tanzania." *American Journal of Biological Anthropology* 185: e25007.

Dryden, I. L., and K. V. Mardia. 1998. *Statistical Shape Analysis*. Wiley.

Dunmore, C. J., M. M. Skinner, A. Bardo, et al. 2020. "The Position of Australopithecus Sediba Within Fossil Hominin Hand Use Diversity." *Nature Ecology & Evolution* 4, no. 7: 911–918. https://doi.org/10.1038/s41559-020-1207-5.

Feix, T., T. L. Kivell, E. Pouydebat, and A. M. Dollar. 2015. "Estimating Thumb-Index Finger Precision Grip and Manipulation Potential in Extant and Fossil Primtes." *Journal of the Royal Society Interface* 12, no. 106: 20150176. https://doi.org/10.1098/rsif.2015.0176.

Feuerriegel, E. M., D. J. Green, C. S. Walker, et al. 2017. "The Upper Limb of Homo Naledi." *Journal of Human Evolution* 104: 155–173. https://doi.org/10.1016/J.JHEVOL.2016.09.013.

Feuerriegel, E. M., J. L. Voisin, S. E. Churchill, et al. 2019. "Upper Limb Fossils of Homo Naledi From the Lesedi Chamber, Rising Star System, South Africa." *PaleoAnthropology*: 311–349. https://hal.archives-ouvertes.fr/hal-02896879.

26927691, 2025, 4, Downloaded from https://onlinelibrary.wiley.com/doi/10.1002/ajpa.70157 by NICE, National Institute for Health and Care Excellence, Wiley Online Library on [09/12/2025]. See the Terms and Conditions (https://onlinelibrary.wiley.com/terms-and-conditions) on Wiley Online Library for rules of use; OA articles are governed by the applicable Creative Commons License

Finestone, E. M., M. H. Brown, S. R. Ross, and H. Pontzer. 2018. "Great Ape Walking Kinematics: Implications for Hominoid Evolution." *American Journal of Physical Anthropology* 166: 43–55. https://doi.org/10.1002/ajpa.23397.

Goodall, C. 1991. "Procrustes Methods in the Statistical Analysis of Shape." *Journal of the Royal Statistical Society. Series B, Statistical Methodology* 53, no. 2: 285–321.

Gower, J. C. 1975. "Generalized Procrustes Analysis." *Psychometrika* 40, no. 1: 33–51.

Granger, D. E., D. Stratford, L. Bruxelles, R. J. Gibbon, R. J. Clarke, and K. Kuman. 2022. "Cosmogenic Nuclide Dating of Australopithecus at Sterkfontein, South Africa." *Proceedings of the National Academy of Sciences of the United States of America* 119, no. 27: e2123516119.

Grosskopf, B. 2015. *Der Vergessene Friedhof.* Universitätsverlag Göttingen. https://doi.org/10.17875/gup2015-884.

Gunz, P., and P. Mitteroecker. 2013. "Semilandmarks: A Method for Quantifying Curves and Surfaces." *Hystrix, the Italian Journal of Mammalogy* 24, no. 1: 103–109.

Hamrick, M. W. 1997. "Functional Osteology of the Primate Carpus With Special Reference to Strepsirhini." *American Journal of Physical Anthropology* 104, no. 1: 105–116.

Hawks, J., M. Elliott, P. Schmid, et al. 2017. "New Fossil Remains of Homo Naledi From the Lesedi Chamber, South Africa." *eLife* 6: e24232. https://doi.org/10.7554/ELIFE.24232.

Hicks, M., and A. Hicks. 2001. "St. Gregory's Priory, Northgate, Canterbury Excavations 1988–1991. Canterbury Archaeological Trust Ltd: Volume II".

Hunt, K. D. 1991. "Mechanical Implications of Chimpanzee Positional Behavior." *American Journal of Physical Anthropology* 86, no. 4: 521–536. https://doi.org/10.1002/AJPA.1330860408;PAGE:STRING:ARTICLE/CHAPTER.

Inouye, S. E. 1994. "Ontogeny of Knuckle-Walking Hand Postures in African Apes." *Journal of Human Evolution* 26, no. 5–6: 459–485. https://doi.org/10.1006/jhev.1994.1028.

Jenkins, F. A., and J. G. Fleagle. 1975. "Knuckle-Walking and the Functional Anatomy of the Wrists in Living Apes." In *Primate Functional Morphology and Evolution*, edited by R. H. Tuttle, 213–227. Mouton.

Karakostis, F. A., G. Hotz, V. Tourloukis, and K. Harvati. 2018. "Evidence of Precision Grasping in Neandertal Daily Activities." *Science Advances* 4: eaat2369.

Kauer, J. M. G., and A. de Lange. 1987. "The Carpal Joint: Anatomy and Function." *Hand Clinics* 3, no. 1: 23–29. https://doi.org/10.1016/S0749-0712(21)00632-6.

Key, A., C. J. Dunmore, K. G. Hatala, and E. M. Williams-Hatala. 2017. "Flake Morphology as a Record of Manual Pressure During Stone Tool Production." *Journal of Archaeological Science: Reports* 12: 43–53.

Key, A. J., and C. J. Dunmore. 2015. "The Evolution of the Hominin Thumb and the Influence Exerted by the Non-Dominant Hand During Stone Tool Production." *Journal of Human Evolution* 78: 60–69.

Kibii, J. M., R. J. Clarke, and M. W. Tocheri. 2011. "A Hominin Scaphoid From Sterkfontein, Member 4: Morphological Description and First Comparative Phenetic 3D Analyses." *Journal of Human Evolution* 61, no. 4: 510–517. https://doi.org/10.1016/J.JHEVOL.2011.06.001.

Kivell, T. L., and D. R. Begun. 2007. "Frequency and Timing of Scaphoid-Centrale Fusion in Hominoids." *Journal of Human Evolution* 52, no. 3: 321–340. https://doi.org/10.1016/j.jhevol.2006.10.002.

Kivell, T. L. 2007. "Ontogeny of the Hominoid Midcarpal Joint and Implications for the Origin of Hominin Bipedalism." PhD Thesis, Toronto, University of Toronto.

Kivell, T., S. Churchill, J. Kibii, P. Schmid, and L. Berger. 2018. "The Hand of *Australopithecus Sediba*." *PaleoAnthropology*: 283–333.

Kivell, T. L. 2015. "Evidence in Hand: Recent Discoveries and the Early Evolution of Human Manual Manipulation." *Philosophical Transactions of the Royal Society, B: Biological Sciences* 370: 20150105. https://doi.org/10.1098/rstb.2015.0105.

Kivell, T. L. 2016. "The Primate Wrist." In *The Evolution of the Primate Hand. Developments in Primatology: Progress and Prospects*, edited by T. Kivell, P. Lemelin, B. Richmond, and D. Schmitt, 17–54. Springer. https://doi.org/10.1007/978-1-4939-3646-5_3.

Kivell, T. L., N. Baraki, V. Lockwood, E. M. Williams-Hatala, and B. A. Wood. 2023. "Form, Function and Evolution of the Human Hand." *American Journal of Biological Anthropology* 181: 6–57. https://doi.org/10.1002/ajpa.24667.

Kivell, T. L., and D. R. Begun. 2009. "New Primate Carpal Bones From Rudabánya (Late Miocene, Hungary): Taxonomic and Functional Implications." *Journal of Human Evolution* 57, no. 6: 697–709.

Kivell, T. L., A. S. Deane, M. W. Tocheri, et al. 2015. "The Hand of *Homo Naledi*." *Nature Communications* 6, no. 1: 1–9. https://doi.org/10.1038/ncomms9431.

Kivell, T. L., J. M. Kibii, S. E. Churchill, P. Schmid, and L. R. Berger. 2011. "*Australopithecus Sediba* Hand Demonstrates Mosaic Evolution of Locomotor and Manipulative Abilities." *Science* 333, no. 6048: 1411–1417. https://doi.org/10.1126/science.1202625.

Kivell, T. L., A. Rosas, A. Estalrrich, et al. 2018. "New Neandertal Wrist Bones From El Sidrón, Spain (1994–2009)." *Journal of Human Evolution* 114: 45–75.

Kivell, T. L., and D. Schmitt. 2009. "Independent Evolution of Knuckle-Walking in African Apes Shows That Humans Did Not Evolve From a Knuckle-Walking Ancestor." *Proceedings of the National Academy of Sciences of the United States of America* 106, no. 34: 14241–14246. https://doi.org/10.1073/PNAS.0901280106.

Kraft, T. S., V. V. Venkataraman, and N. J. Dominy. 2014. "A Natural History of Human Tree Climbing." *Journal of Human Evolution* 71: 105–118.

Larson, S. G. 1996. "Estimating Humeral Torsion on Incomplete Fossil Anthropoid Humeri." *Journal of Human Evolution* 31, no. 3: 239–257. https://doi.org/10.1006/JHEV.1996.0059.

Larson, S. G. 2009. "Evolution of the Hominin Shoulder: Early Homo." In *Vertebrate Paleobiology and Paleoanthropology*, 65–75. Springer. https://doi.org/10.1007/978-1-4020-9980-9_7.

Lewis, O. J. 1989. *Functional Morphology of the Evolving Hand and Foot*. Clarendon Press.

Lockwood, C. A., and P. v. Tobias. 2002. "Morphology and Affinities of New Hominin Cranial Remains From Member 4 of the Sterkfontein Formation, Gauteng Province, South Africa." *Journal of Human Evolution* 42, no. 4: 389–450. https://doi.org/10.1006/JHEV.2001.0532.

Loeffelbein, D. J., L. M. Ritschl, A. Rau, et al. 2015. "Analysis of Computer-Aided Techniques for Virtual Planning in Nasoalveolar Moulding." *British Journal of Oral and Maxillofacial Surgery* 53, no. 5: 455–460. https://doi.org/10.1016/j.bjoms.2015.03.002.

Lorenzo, C., J. L. Arsuaga, and J. M. Carretero. 1999. "Hand and Foot Remains From the Gran Dolina Early Pleistocene Site (Sierra de Atapuerca, Spain)." *Journal of Human Evolution* 37, no. 3–4: 501–522.

Lovejoy, C. O., S. W. Simpson, T. D. White, B. Asfaw, and G. Suwa. 2009. "Careful Climbing in the Miocene: The Forelimbs of Ardipithecus Ramidus and Humans Are Primitive." *Science* 326, no. 5949: 70.

Marzke, M. W. 1971. "Origin of the Human Hand." *American Journal of Physical Anthropology* 34: 61–84.

Marzke, M. W. 1997. "Precision Grips, Hand Morphology, and Tools." *American Journal of Physical Anthropology* 102, no. 1: 91–110. https://

26927691, 2025, 4, Downloaded from https://onlinelibrary.wiley.com/doi/10.1002/ajpa.70157 by NICE, National Institute for Health and Care Excellence, Wiley Online Library on [09/12/2025]. See the Terms and Conditions (https://onlinelibrary.wiley.com/terms-and-conditions) on Wiley Online Library for rules of use; OA articles are governed by the applicable Creative Commons License

doi.org/10.1002/(SICI)1096-8644(199701)102:1<91::AID-AJPA8>3.0.CO;2-G.

Marzke, M. W., R. F. Marzke, R. L. Linscheid, et al. 1999. "Chimpanzee Thumb Muscle Cross Sections, Moment Arms and Potential Torques, and Comparisons With Humans." *American Journal of Physical Anthropology* 110, no. 2: 163–178. https://doi.org/10.1002/(SICI)1096-8644(199910)110:2<163::AID-AJPA4>3.0.CO;2-A.

Marzke, M. W. 2013. "Tool Making, Hand Morphology and Fossil Hominins." *Philosophical Transactions of the Royal Society, B: Biological Sciences* 368, no. 1630: 20120414.

Marzke, M. W., L. F. Marchant, W. C. McGrew, and S. P. Reece. 2015. "Grips and Hand Movements of Chimpanzees During Feeding in Mahale Mountains National Park, Tanzania." *American Journal of Physical Anthropology* 156, no. 3: 317–326. https://doi.org/10.1002/ajpa.22651.

Marzke, M. W., and R. F. Marzke. 2000. "Evolution of the Human Hand: Approaches to Acquiring, Analysing and Interpreting the Anatomical Evidence." *Journal of Anatomy* 197, no. 1: 121–140. https://doi.org/10.1046/J.1469-7580.2000.19710121.X.

Marzke, M. W., K. L. Wullstein, and S. F. Viegas. 1992. "Evolution of the Power ("Squeeze") Grip and Its Morphological Correlates in Hominids." *American Journal of Physical Anthropology* 89, no. 3: 283–298.

Matarazzo, S. 2013. "Manual Pressure Distribution Patterns of Knuckle-Walking Apes." *American Journal of Physical Anthropology* 152, no. 1: 44–50. https://doi.org/10.1002/AJPA.22325.

Moggi-Cecchi, J., and S. Roscoe, eds. 2014. "Il Museo di Storia Naturale dell'Università degli Studi di Firenze." In *Etonologiche/the Museum of Natural History of the University of Florence. The Anthropological and Ethnological Collections*, Le collezioni antropologiche ed. Firenze University Press.

Moggi-Moojen, T. M., J. G. Snel, M. J. P. F. Ritt, H. W. Venema, J. M. G. Kauer, and K. E. Bos. 2003. "In Vivo Analysis of Carpal Kinematics and Comparative Review of the Literature." *Journal of Hand Surgery* 28, no. 1: 81–87. https://doi.org/10.1053/jhsu.2003.50009.

Napier, J. R. 1956. "The Prehensile Movements of the Human Hand." *Journal of Bone and Joint Surgery British* 38 B, no. 4: 902–913. https://doi.org/10.1302/0301-620x.38b4.902.

Napier, J. R. 1960. "Studies of the Hands of Living Primates." *Proceedings of the Zoological Society of London* 134, no. 4: 647–657. https://doi.org/10.1111/j.1469-7998.1960.tb05606.x.

Neufuss, J., M. M. Robbins, J. Baeumer, T. Humle, and T. L. Kivell. 2017. "Comparison of Hand Use and Forelimb Posture During Vertical Climbing in Mountain Gorillas (*Gorilla beringei beringei*) and Chimpanzees (*Pan troglodytes*)." *American Journal of Physical Anthropology* 164, no. 4: 651–664.

Neufuss, J., M. M. Robbins, J. Baeumer, T. Humle, and T. L. Kivell. 2019. "Manual Skills for Food Processing by Mountain Gorillas (*Gorilla beringei beringei*) in Bwindi Impenetrable National Park, Uganda." *Biological Journal of the Linnean Society* 127, no. 3: 543–562. https://doi.org/10.1093/biolinnean/bly071.

Niewoehner, W. A. 2001. "Behavioral Inferences From the Skhul/Qafzeh Early Modern Human Hand Remains." *Proceedings of the National Academy of Sciences of the United States of America* 98, no. 6: 2979–2984.

Niewoehner, W. A., A. H. Weaver, and E. Trinkaus. 1997. "Neandertal Capitate-Metacarpal Articular Morphology." *American Journal of Physical Anthropology* 103, no. 2: 219–233.

Niewoehner, W. A. 2006. "Neanderthal Hands in Their Proper Perspective." In *Vertebrate Paleobiology and Paleoanthropology* Issue 9781402051203, 157–190. Springer. https://doi.org/10.1007/978-1-4020-5121-0_9.

Orr, C. M. 2005. "Knuckle-Walking Anteater: A Convergence Test of Adaptation for Purported Knuckle-Walking Features of African Hominidae." *American Journal of Physical Anthropology* 128, no. 3: 639–658. https://doi.org/10.1002/AJPA.20192.

Orr, C. M. 2010. *Adaptations to Knuckle-Walking and Digitigrady: A Three-Dimensional Kinematic and Morphometry Analysis of the Anthropoid Wrist*. Arizona State University.

Orr, C. M., M. W. Tocheri, S. E. Burnett, et al. 2013. "New Wrist Bones of Homo Floresiensis From Liang Bua (Flores, Indonesia)." *Journal of Human Evolution* 64, no. 2: 109–129. https://doi.org/10.1016/j.jhevol.2012.10.003.

Orr, C. M. 2018. "Kinematics of the Anthropoid Os Centrale and the Functional Consequences of Scaphoid-Centrale Fusion in African Apes and Hominins." *Journal of Human Evolution* 114: 102–117. https://doi.org/10.1016/j.jhevol.2017.10.002.

Pickering, R., P. H. Dirks, Z. Jinnah, et al. 2011. "*Australopithecus Sediba* at 1.977 ma and Implications for the Origins of the Genus *Homo*." *Science* 333, no. 6048: 1421–1423. https://doi.org/10.1126/SCIENCE.1203697/SUPPL_FILE/PICKERING-SOM.PDF.

Pickering, R., and A. I. Herries. 2020. "A New Multidisciplinary Age of 2.61–2.07 ma for the Sterkfontein Member 4 Australopiths." In *Hominin Postcranial Remains From Sterkfontein, South Africa, 1936–1995*, edited by B. Zipfel, B. G. Richmond, and C. V. Ward, 21–30. Oxford University Press.

Püschel, T. A., J. Marcé-Nogué, A. T. Chamberlain, A. Yoxall, and W. I. Sellers. 2020. "The Biomechanical Importance of the Scaphoid-Centrale Fusion During Simulated Knuckle-Walking and Its Implications for Human Locomotor Evolution." *Scientific Reports* 10, no. 1: 3526. https://doi.org/10.1038/s41598-020-60590-6.

R Core Team. 2021. *R: A Language and Environment for Statistical Computing*. R Foundation for Statistical Computing. https://www.R-project.org/.

Remis, M. 1995. "Effects of Body Size and Social Context on the Arboreal Activities of Lowland Gorillas in the Central African Republic." *American Journal of Physical Anthropology* 97, no. 4: 413–433. https://doi.org/10.1002/AJPA.1330970408.

Richmond, B. G., D. R. Begun, and D. S. Strait. 2001. "Origin of Human Bipedalism: The Knuckle-Walking Hypothesis Revisited." *American Journal of Physical Anthropology* 116, no. S33: 70–105. https://doi.org/10.1002/AJPA.10019.

Richmond, B. G., and D. S. Strait. 2001. "Knuckle-Walking Hominid Ancestor: A Reply to Corruccini & McHenry." *Journal of Human Evolution* 40: 513–520.

Robbins, J. L., P. H. Dirks, E. M. Roberts, et al. 2021. "Providing Context to the Homo Naledi Fossils: Constraints From Flowstones on the Age of Sediment Deposits in Rising Star Cave, South Africa." *Chemical Geology* 567: 120,108.

Robbins, M. M., R. C. Drummond-Clarke, A. M. Robbins, K. R. Ostrofsky, and T. L. Kivell. 2025. "Gorillas Are Arboreal Apes." *Current Biology* 35, no. 12: 2974–2979.

Robinson, C., and C. E. Terhune. 2017. "Error in Geometric Morphometric Data Collection: Combining Data From Multiple Sources." *American Journal of Physical Anthropology* 164: 62–75.

Rohde, R. S., J. J. Crisco, and S. W. Wolfe. 2010. "The Advantage of Throwing the First Stone: How Understanding the Evolutionary Demands of *Homo sapiens* Is Helping Us Understand Carpal Motion." *Journal of the American Academy of Orthopaedic Surgeons* 18, no. 1: 51–58.

Rohlf, F. J., and D. Slice. 1990. "Extensions of the Procrustes Method for the Optimal Superimposition of Landmarks." *Systematic Biology* 39: 40–59.

26927691, 2025, 4, Downloaded from https://onlinelibrary.wiley.com/doi/10.1002/ajpa.70157 by NICE, National Institute for Health and Care Excellence, Wiley Online Library on [09/12/2025]. See the Terms and Conditions (https://onlinelibrary.wiley.com/terms-and-conditions) on Wiley Online Library for rules of use; OA articles are governed by the applicable Creative Commons License

Sala, N., I. Martínez, C. Lorenzo, et al. 2024. "Taphonomic Skeletal Disturbances in the Sima de los Huesos Postcranial Remains." *Anatomical Record* 307, no. 7: 2437–2450.

Samuel, D. S., S. Nauwelaerts, J. M. G. Stevens, and T. L. Kivell. 2018. "Hand Pressures During Arboreal Locomotion in Captive Bonobos (*Pan paniscus*)." *Journal of Experimental Biology* 221, no. 8: jeb170910. https://doi.org/10.1242/jeb.170910.

Sarmiento, E. E. 1988. "Anatomy of the Hominoid Wrist Joint: Its Evolutionary and Functional Implications." *International Journal of Primatology* 9, no. 4: 281–345. https://doi.org/10.1007/BF02737381.

Sarringhaus, L. A., L. M. MacLatchy, and J. C. Mitani. 2014. "Locomotor and Postural Development of Wild Chimpanzees." *Journal of Human Evolution* 66: 29–38.

Schlager, S. 2017. "Morpho and Rvcg—Shape Analysis in R: R-Packages for Geometric Morphometrics, Shape Analysis and Surface Manipulations." In *Statistical Shape and Deformation Analysis: Methods, Implementation and Applications*, edited by G. Zheng, S. Li, and G. Szekely, 217–256. Academic Press. https://doi.org/10.1016/B978-0-12-810493-4.00011-0.

Schwarcz, H. P., W. M. Buhay, R. Grün, et al. 1989. "ESR Dating of the Neanderthal Site, Kebara Cave, Israel." *Journal of Archaeological Science* 16, no. 6: 653–659. https://doi.org/10.1016/0305-4403(89)90029-0.

Schwarcz, H. P., J. J. Simpson, and C. B. Stringer. 1998. "Neanderthal Skeleton From Tabun: U-Series Data by Gamma-Ray Spectrometry." *Journal of Human Evolution* 35, no. 6: 635–645. https://doi.org/10.1006/JHEV.1998.0252.

Shearer, B. M., S. B. Cooke, L. B. Halenar, et al. 2017. "Evaluating Causes of Error in Landmark-Based Data Collection Using Scanners." *PLoS One* 12: e0187452.

Soressi, M., S. P. McPherron, M. Lenoir, et al. 2013. "Neandertals Made the First Specialized Bone Tools in Europe." *Proceedings of the National Academy of Sciences of the United States of America* 110, no. 35: 14186–14190.

Sparacello, V., S. Rossi, P. Pettitt, C. Roberts, J. Salvatore, and V. Formicola. 2018. "New Insights on Final Epigravettian Funerary Behaviour at Arene Candide Cave (Western Liguria, Italy) From Osteological and Spatial Analysis of Secondary Bone Deposits." *Journal of Anthropological Sciences* 96: 1–24.

Sparacello, V. S., I. Dori, S. Rossi, et al. 2021. "New Human Remains From the Late Epigravettian Necropolis of Arene Candide (Liguria, Northwestern Italy): Direct Radiocarbon Evidence and Inferences on the Funerary Use of the Cave During the Younger Dryas." *Quaternary Science Reviews* 268: 107131. https://doi.org/10.1016/J.QUASCIREV.2021.107131.

Syeda, S. M., C. J. Dunmore, M. M. Skinner, et al. 2025. "Phalangeal Cortical Bone Distribution Reveals Different Dexterous and Climbing Behaviors in *Australopithecus Sediba* and *Homo Naledi*." *Science Advances* 11, no. 20: eadt1201. https://doi.org/10.1126/sciadv.adt1201.

Tallman, M. 2012. "Morphology of the Distal Radius in Extant Hominoids and Fossil Hominins: Implications for the Evolution of Bipedalism." *Anatomical Record: Advances in Integrative Anatomy and Evolutionary Biology* 295, no. 3: 454–464. https://doi.org/10.1002/ar.22405.

Tarrega-Saunders, E. L., C. King, A. M. Roberts, and S. K. Thorpe. 2021. "Knuckle-Walking and Behavioural Flexibility in Great Apes." *Revue de Primatologie* 12.

Taverne, M., A. C. Fabre, M. Herbin, et al. 2018. "Convergence in the Functional Properties of Forelimb Muscles in Carnivorans: Adaptations to an Arboreal Lifestyle?" *Biological Journal of the Linnean Society* 125, no. 2: 250–263. https://doi.org/10.1093/BIOLINNEAN/BLY123.

Thompson, N. E. 2020. "The Biomechanics of Knuckle-Walking: 3-D Kinematics of the Chimpanzee and Macaque Wrist, Hand and Fingers." *Journal of Experimental Biology* 223, no. 14: 224. https://doi.org/10.1242/JEB.224360.

Thompson, N. E., K. R. Ostrofsky, S. C. McFarlin, M. M. Robbins, T. S. Stoinski, and S. Almécija. 2018. "Unexpected Terrestrial Hand Posture Diversity in Wild Mountain Gorillas." *American Journal of Physical Anthropology* 166, no. 1: 84–94. https://doi.org/10.1002/AJPA.23404.

Tocheri, M. W., M. W. Marzke, D. Liu, et al. 2003. "Functional Capabilities of Modern and Fossil Hominid Hands: Three-Dimensional Analysis of Trapezia." *American Journal of Physical Anthropology* 122, no. 2: 101–112. https://doi.org/10.1002/ajpa.10235.

Tocheri, M. W. 2007. *Three-Dimensional Riddles of the Radial Wrist: Derived Carpal and Carpometacarpal Joint Morphology in the Genus Homo and the Implications for Understanding the Evolution of Stone Tool-Related Behaviors in Hominins*. Arizona State University.

Tocheri, M. W., C. M. Orr, M. C. Jacofsky, and M. W. Marzke. 2008. "The Evolutionary History of the Hominin Hand Since the Last Common Ancestor of Pan and Homo." *Journal of Anatomy* 212, no. 4: 544–562. https://doi.org/10.1111/j.1469-7580.2008.00865.x.

Tocheri, M. W., C. M. Orr, S. G. Larson, et al. 2007. "The Primitive Wrist of *Homo Floresiensis* and Its Implications for Hominin Evolution." *Science* 317, no. 5845: 1743–1745. https://doi.org/10.1126/science.1147143.

Tocheri, M. W., C. R. Solhan, C. M. Orr, et al. 2011. "Ecological Divergence and Medial Cuneiform Morphology in Gorillas." *Journal of Human Evolution* 60: 171–184.

Trinkaus, E. 1983. *The Shanidar Neanderthals*. Academic Press.

Trinkaus, E., ed. 1989. *The Emergence of Modern Humans: Biocultural Adaptations in the Later Pleistocene*. Cambridge University Press.

Tuttle, H. R. 1985. "The Positional Behavior and Adaptive Complexes of Pan Gorilla." In *Primate Morphophysiology, Locomotor Analysis and Human Bipedalism*. Tokyo University Press. https://ci.nii.ac.jp/naid/10016063828.

Tuttle, R. H. 1969. "Quantitative and Functional Studies on the Hands of the Anthropoidea. I. The Hominoidea." *Journal of Morphology* 128, no. 3: 309–363. https://doi.org/10.1002/JMOR.1051280304.

van Lawick-Goodall, J. 1968. "The Behaviour of Free-Living Chimpanzees in the Gombe Stream Reserve." *Animal Behaviour Monographs* 1: 161–311. https://doi.org/10.1016/s0066-1856(68)80003-2.

Vrba, E. S. 1979. "A New Study of the Scapula of *Australopithecus Africanus* From Sterkfontein." *American Journal of Physical Anthropology* 51, no. 1: 117–129. https://doi.org/10.1002/AJPA.1330510114.

Waltenberger, L., K. Rebay-Salisbury, and P. Mitteroecker. 2021. "Three-Dimensional Surface Scanning Methods in Osteology: A Topographical and Geometric Morphometric Comparison." *American Journal of Physical Anthropology* 174: 846–858.

Wolfe, S. W., J. J. Crisco, C. M. Orr, and M. W. Marzke. 2006. "The Dart-Throwing Motion of the Wrist: Is It Unique to Humans?" *Journal of Hand Surgery* 31, no. 9: 1429–1437. https://doi.org/10.1016/J.JHSA.2006.08.010.

Wood, R. E., T. F. Higham, T. De Torres, et al. 2013. "A New Date for the Neanderthals From El Sidrón Cave (Asturias, Northern Spain)." *Archaeometry* 55, no. 1: 148–158. https://doi.org/10.1111/J.1475-4754.2012.00671.X.

Wunderlich, R. E., and W. L. Jungers. 2009. "Manual Digital Pressures During Knuckle-Walking in Chimpanzees (*Pan troglodytes*)." *American Journal of Physical Anthropology* 139, no. 3: 394–403. https://doi.org/10.1002/ajpa.20994.

Zihlman, A. L. 1984. "Body Build and Tissue Composition in *Pan paniscus* and *Pan troglodytes*, With Comparisons to Other Hominoids." In *The Pygmy Chimpanzee*, edited by R. l. Susman, 179–200. Springer.

26927691, 2025, 4, Downloaded from https://onlinelibrary.wiley.com/doi/10.1002/ajpa.70157 by NICE, National Institute for Health and Care Excellence, Wiley Online Library on [09/12/2025]. See the Terms and Conditions (https://onlinelibrary.wiley.com/terms-and-conditions) on Wiley Online Library for rules of use; OA articles are governed by the applicable Creative Commons License

Zihlman, A. L., and D. L. Cramer. 1978. "Skeletal Differences Between Pygmy (*Pan paniscus*) and Common Chimpanzees (*Pan troglodytes*)." *Folia Primatologica* 29: 86–89.

Supporting Information

Additional supporting information can be found online in the Supporting Information section. **Table S1:** Specimens included in extant study sample. **Table S2:**. Summary of scanning methods for sample. **Table S3:**. Permutation tests for centroid size, with distances between variances shown. Bold indicates (p values) of ($p < 0.05$). Abbreviations are Gg *(Gorilla gorilla)*, Pp *(Pan paniscus)*, Pt *(Pan troglodytes)*, Hs (*Homo sapiens*). **Figure S1:**. Original and reconstructed surface models of *H. naledi* U.W. 101-1726 scaphoid tubercle. The U.W. 101-1726 trapezium-trapezoid facet was extended palmarly and the base of tubercle was made more robust to match the Lesedi specimen. A second reconstruction of U.W. 101-1726 was made with a more extended, ape-like tubercle, with minimal changes to the trapezium-trapezoid facet. **Figure S2:**. Original and reconstructed surface models of Neandertal Tabun C1 scaphoid tubercle. We reconstructed the tubercle in two different ways based on the morphology of the other Neandertal specimens, with one reconstruction having a slightly more robust and more extended tubercle than the other. **Figure S3:**. PCA plot of intraobserver error test of both the anatomical landmarks and curve sliding semi-landmarks repeated five times on three *P. troglodytes* specimens. **Figure S4:**. PCA plot of interobserver error test of scaphoid main and curve sliding landmarks on three *P. troglodytes* specimens, with the landmarks carried out by another individual denoted in a darker shade.

26927691, 2025, 4, Downloaded from https://onlinelibrary.wiley.com/doi/10.1002/ajpa.70157 by NICE, National Institute for Health and Care Excellence, Wiley Online Library on [09/12/2025]. See the Terms and Conditions (https://onlinelibrary.wiley.com/terms-and-conditions) on Wiley Online Library for rules of use; OA articles are governed by the applicable Creative Commons License